siRNA-mediated gene knockdown via electroporation in hydrozoan jellyfish embryos

[1] Tokiha Masuda-Ozawa, [2] Sosuke Fujita, [3] Ryotaro Nakamura, [3] Hiroshi Watanabe, [2] Erina Kuranaga, and [1,4] Yu-ichiro Nakajima*

1. Frontier Research Institute for Interdisciplinary Sciences, Tohoku University, Sendai, Japan
2. Graduate School of Life Sciences, Tohoku University, Sendai, Japan
3. Evolutionary Neurobiology Unit, Okinawa Institute of Science and Technology Graduate University, Okinawa, Japan
4. Graduate School of Pharmaceutical Sciences, The University of Tokyo

*Author for correspondence e-mail: nakaji97@g.ecc.u-tokyo.ac.jp
Tel: +81-3-5841-4863

Running title: **siRNA gene knockdown in jellyfish embryos**
Main text: 4361 words (Abstract: 247 words)
Figures: 6 **Supplementary information** (Figures: 5; Table: 2)
Keywords: siRNA, electroporation, cnidarian, hydrozoan, jellyfish, *Clytia, Cladonema*

Abstract

As the sister group to bilaterians, cnidarians stand in a unique phylogenetic position that provides insights into evolutionary aspects of animal development, physiology, and behavior. While cnidarians are classified into two types, sessile polyps and free-swimming medusae, most studies at the cellular and molecular levels have been conducted on representative polyp-type cnidarians and have established techniques of genetic manipulation. Recently, gene knockdown by delivery of short hairpin RNAs into eggs via electroporation has been introduced to two polyp-type cnidarians, *Nematostella vectensis* and *Hydractinia symbiolongicarpus*, enabling systematic loss-of-function experiments. By contrast, current methods of genetic manipulation for medusa-type cnidarians, or jellyfish, are quite limited, and reliable techniques are required to interrogate function of specific genes. Here, we present a method to knockdown target genes by small interfering RNA (siRNA) delivery into fertilized eggs via electroporation, using the hydrozoan jellyfish, *Clytia hemisphaerica* and *Cladonema paciificum*. We show that siRNAs targeting endogenous *GFP1* and *Wnt3* in *Clytia* efficiently knockdown gene expression and result in known planula phenotypes: loss of green fluorescence and defects in axial patterning, respectively. We also successfully knock down endogenous *Wnt3* in *Cladonema* by siRNAs electroporation, which circumvents the technical difficulty of microinjecting small eggs. Unexpectedly, *Wnt3* knockdown in *Cladonema* does not induce morphological defects in planula, suggesting a distinct mechanism that operates during embryogenesis. Our method for electroporation of siRNAs targeting specific genes is applicable to other animals, including and beyond jellyfish species, and will facilitate the investigation and understanding of myriad aspects of animal development.

Introduction

The phylum Cnidaria, as the sister group to Bilateria, separated from their common ancestor over 500 million years ago. Cnidarians have diversified their morphologies in the forms of corals, sea anemones, hydroids, and jellyfish, all of which are divided into two clades, Anthozoa and Medusozoa; The two differ in that Anthozoa includes only sessile polyp-type animals, while Medusozoa (Hydrozoa, Staurozoa, Scyphozoa, and Cubozoa) includes two forms: polyp and medusa, or jellyfish stage (Fig. 1A)[1,2]. The life cycle of most, though not all, jellyfish includes five forms: gametes, fertilized eggs, planulae, polyps, and medusae[3]. Fertilized eggs undergo embryogenesis to become planula larvae, which metamorphose into sessile polyps. While vegetatively-growing polyps give rise to free-swimming medusae through the process of budding or strobilization, medusae sexually reproduce by releasing gametes. Due to their unique phylogenetic position, studies using cnidarians have provided evolutionary insights into development, regeneration, and behaviors in multicellular animals[1,4,5]. To date, the field's molecular and cellular understanding of cnidarians has been acquired primarily using polyp-type animals such as the anthozoan *Nematostella vectensis* and the hydrozoan *Hydra* and *Hydractinia*. By contrast, jellyfish biology remains largely unestablished.

Among jellyfish species, the hydrozoan *Clytia hemisphaerica* is the best-studied laboratory model[6,7]. The well-established method for maintaining and propagating animals ensures a reliable resource for daily experiments[8]. While the transparent and small-sized medusae allow the whole-mount visualization, relatively large-sized eggs (~180 μm diameter) enable different manipulations with microinjection (Fig. 1B). Indeed, gene silencing by morpholino oligos and mRNA microinjection as well as gene knockout via CRISPR/Cas9 allow for the investigation of the functions of genes of interest[9-13]. Furthermore, the *Clytia* genome assembly is complete, and transcriptome profiles are available for various stages and tissues, even at the single-cell level, which creates the foundation for research at the molecular level[12,14-18]. These resources and techniques, together with recently-established transgenesis[19], accelerate research into different features associated with distinct *Clytia* life stages. Current research topics using *Clytia* range from the establishment of the oral-aboral axis during embryogenesis and

95 gametogenesis regulated by the light-dark cycle to body regeneration, nervous system
96 development, and characterizing adult medusa behavior[9,10,12,17,19,20].
97 By contrast, the hydrozoan *Cladonema pacificum* is an emerging model jellyfish
98 that has been recently utilized for various studies in development, regeneration, and
99 physiology[21]. The ease of rearing all stages of *Cladonema* without a filtration system or
100 large water tank, along with their high spawning rate, enables easy lab maintenance.
101 The small-sized medusae with branched tentacles allow for investigations of body size
102 control and tentacle morphogenesis (Fig. 1C)[22-24]. *Cladonema* gametogenesis is
103 regulated by the light-dark cycle as in *Clytia*, and recent work has identified the
104 neuropeptides involved in oocyte maturation[25]. Furthermore, *Cladonema* medusae
105 possess primitive complex eyes (ocelli) in their tentacle bulbs, and studies using the
106 closely related species *Cladonema radiatum* have identified conserved light-sensitive
107 opsins and regulators of eye formation (*Pax*, *Six*, and *Eya*)[25-29], providing a model for
108 the evolutionary developmental biology of photoreceptor organs. Despite these
109 attractive features of *Cladonema* as a laboratory animal, no genome assembly or
110 transcriptome is currently available, and genetic manipulation techniques are only just
111 being developed. One major technical issue in manipulating *Cladonema* is their small
112 eggs—with a diameter of approximately 60 μm (Fig. 1C), regular microinjection is quite
113 difficult. Establishing genetic manipulations is required to facilitate the in-depth
114 investigations needed to further understand the biology of *Cladoenema*, and an
115 alternative method that eliminates need for microinjection would greatly facilitate that
116 objective.
117 RNA interference (RNAi), the phenomenon of double stranded RNA (dsRNA)
118 mediated silencing of target genes, has been widely exploited in living organisms to
119 analyze gene function[30], primarily using chemically- or *in vitro*-synthesized double-
120 stranded small interfering RNAs (siRNAs) or vector-based short hairpin RNAs
121 (shRNAs)[31]. In cnidarians, siRNA-mediated gene silencing was initially applied to
122 *Nematostella* and *Hydra* polyps via soaking or electroporation[32-34]. Additionally, gene
123 knockdown via shRNA microinjection or electroporation into eggs has recently been
124 utilized in studies using *Nematostella* and *Hydractinia* to show efficient reduction in
125 gene expression and associated phenotypes in early developmental stages[35-38]. In
126 particular, shRNA delivery via electroporation, which does not require the rigors of

127 microinjection, allows for the experimental gene knockdown of large numbers of
128 individuals simultaneously[36,38], opening up the possibility of manipulating genes in
129 different aquatic animals, even those that produce very small eggs like *Cladonema*.
130 The mechanism of RNAi-mediated gene repression after introducing foreign
131 dsRNA into cells involves the microRNA (miRNA) pathway, an endogenous gene
132 repression machinery conserved in both animals and plants[39]. In cnidarians, the
133 presence of the miRNA pathway has been demonstrated in *Nematostella* and
134 *Hydra*[32,40,41]. However, little is known about the endogenous RNAi pathway, especially
135 the presence and roles of miRNAs and the miRNA-related genes, in jellyfish such as
136 *Clytia* and *Cladonema*. Furthermore, in mammalian cultured cells, siRNAs can induce
137 gene repression independent of endogenous dsRNA processing factors, while shRNAs
138 cannot[42,43]. On this basis, we elected to use siRNA instead of shRNA for gene
139 knockdown to avoid the potential pitfall of dsRNA processing in jellyfish.
140 Here we report a gene knockdown method for jellyfish embryos with siRNA via
141 electroporation. Using two hydrozoan species, *Clytia hemisphaerica* and *Cladonema*
142 *pacificum*, we demonstrate that siRNA delivery into fertilized eggs effectively reduces
143 the expression of endogenous genes. We also confirm the known loss-of-function
144 phenotypes in *Clytia* after knocking down *GFP1* or *Wnt3*, which are induced in a dose-
145 dependent manner with siRNA. We further show that knockdown of *Wnt3* in *Cladonema*
146 embryos does not cause defects in planula morphology, implicating a potentially distinct
147 embryogenesis regulating mechanism between these two hydrozoan species. Overall,
148 our siRNA-mediated knockdown approach allows for the manipulation of a large number
149 of embryos through electroporation and enables functional analysis of early
150 development, providing a new experimental platform applicable to different jellyfish
151 species and other marine invertebrates.
152
153
154 ## Materials and Methods
155
156 **Animal culture and spawning induction**
157 *Clytia hemisphaerica* (Z11, Z4B as females and Z4C2, Z23 as males) and *Cladonema*
158 *pacificum* (6W as females and UN2 as males) were used for this research.

159 *Clytia hemisphaerica* were cultured using a previously reported method[8] with a
160 few modifications. Artificial sea water (ASW) was prepared using 220 g SEA LIFE
161 (Marin Tech) per 5L MilliQ water (Merk Millipore) with antibiotics (40 units/ml of penicillin
162 and 40 µg/ml of streptomycin). Medusae, embryos, and planula larvae were maintained
163 at 20ºC. Medusae were fed everyday with Vietnamese brine shrimp (A&A Marine LLC,
164 Elk Rapids, MI, USA). Spawning timing was controlled by a 13 hours (h) dark /11 h light
165 cycle, and spawning was induced by light. Male and female medusae were transferred
166 into V-7 cups (AS ONE) before spawning (60 min for male and 90 min for female after
167 light stimulation).
168 *Cladonema pacificum* were cultured as previously described[23]. *Cladonema*
169 medusae were maintained at 22ºC in ASW, which was prepared by SEA LIFE (Marin
170 Tech) dissolved in tap water with chlorine neutralizer (Coroline off, GEX Co. ltd) (24
171 p.p.t) and antibiotics (40 units/ml penicillin and 40 µg/ml of streptomycin). Spawning
172 timing was controlled by a 30 min dark/23.5 h light cycle, and spawning of male and
173 female gametes was induced by dark stimulation. Before dark stimulation, adult females
174 and males were separately transferred into V7 cups (AS ONE) and 60 mm dishes (BD),
175 respectively.
176 *Nematostella vectensis* were cultured as previously described[44], with a few
177 modifications. Briefly, adult animals were maintained in brackish water at a salinity one-
178 third of artificial seawater (35 g/l, pH 7.5-8.0, SEA LIFE, Marin Tech) and fed with
179 freshly hatched artemia two times per week. Spawning induction was performed at 26°C
180 under light for at least 11 h.
181
182
183 **siRNA and shRNA**
184 siRNA sequences were designed based on CDS sequences and synthesized by
185 manufacturers (Nippon gene Co.Ltd and Sigma-Aldrich, Merk). shRNAs were
186 synthesized as described in previous reports[36,38]. Briefly, shRNAs were synthesized by
187 *in vitro* transcription (IVT) from double stranded DNA templates using the
188 AmpliScribeTM T7-flashTM transcription kit (Lucigen, Inc.) and were purified using
189 Direct-Zol TM RNA Miniprep kits (Zymo Research, R2070). Concentrations of shRNAs
190 were measured by NanoDrop One (Thermo fisher).

191
192
193 **Collection of gametes and electroporation for *Clytia* and *Cladonema* fertilized**
194 **eggs**
195 For preparation of gametes, sexually-mature *Clytia* medusae were treated following a
196 previously reported method[8], partially modified to fit our experimental equipment. Adult
197 medusae were maintained on a 13 h dark/11 h light cycle, and light stimuli induced
198 gametogenesis in 60 min for sperms and 90 min for eggs (Fig. 2A). For *Cladonema*
199 *pacificum*, sexually-mature medusae were maintained on a 30 min dark/23.5 h light
200 cycle. Dark stimulation induced gametogenesis in 25 min. Unfertilized eggs were
201 collected and resuspended in 15% Ficoll (Nacalai tesque, Japan) in ASW to prevent the
202 eggs settling from at the bottom of the microtube or sticking to the microtube surface,
203 keeping the egg solution homogeneous (Fig. 2B)[36,38].
204 Unfertilized *Clytia* and *Cladonema* eggs were collected in dishes and transferred
205 into 1.5 ml tubes coated with Ficoll (Nacalai tesque, Japan) to prevent the eggs from
206 sticking to the tubes. Sperm water was added into eggs, and eggs and sperm were
207 incubated for 5 min at room temperature (20-22ºC). The sperm water was then
208 removed, and fertilized eggs were resuspended in 15% Ficoll in ASW, at which point
209 siRNAs or shRNAs were added into fertilized egg solution. The fertilized eggs and RNA
210 mixture were carefully transferred into a 4 mm cuvette and placed into the shockpod
211 cuvette chamber connected to the Gene Pulser Xcell (Bio-Rad). In most experiments,
212 the Gene Pulser Xcell was used for pulsing with a square wave voltage of 50 V and a
213 single pulse duration of 25 ms, except for optimizing electroporation conditions
214 (Supplementary Figs 1-2). After electroporation, fertilized eggs were transferred to a
215 dish, and incubated for 10 min. The 15% Ficoll solution was removed and replaced with
216 new ASW, and the samples were incubated at 20-22ºC.
217
218
219 **Collection of egg sacs, dejellying, and electroporation for *Nematostella* fertilized**
220 **eggs**
221 The collection of egg sacs, dejellying, and electroporation steps were performed as
222 previously described[36] with several modifications. Briefly, unfertilized egg sacs were

223 incubated in culture media with sperm at 20-25ºC for 30 min. The fertilized egg sacs
224 were then dejellied in freshly prepared L-Cysteine solution (0.04 g/ml, Nacalai tesque, in
225 brackish water; pH adjusted by 5N NaOH at 7.5-8.0) on a shaker for 10 min. The
226 dejellied eggs were rinsed with brackish water before they were suspended in Ficoll
227 solution (Sigma-Aldrich, in brackish water) at final concentrations of 15%. The
228 suspended eggs and siRNA (5 µg/µl stock solution, in MilliQ) were transferred to a 4
229 mm cuvette (Bio-Rad) at the final volume of 200 µl and were gently mixed. The Bio-rad
230 Gene Pulser Xcell was used for pulsing with a square wave voltage of 50 V and a pulse
231 duration of 25 ms. The samples were transferred to a 100 mm dish and maintained in
232 brackish water for 3 days.
233
234
235 **Imaging**
236 GFP and Rhodamine fluorescent imaging and bright field imaging were taken with an
237 Axio Zoom V16 (ZEISS), and image processing was done with ZEN 3.4 blue edition
238 (ZEISS) and Fiji/ImageJ software[45]. Intensity of mean values of green fluorescence was
239 measured using the average brightness (pixel value) of the pixels. To prevent planula
240 movement, we added 0.5 M sodium azide (final concentration was less than 0.25M).
241
242
243 **Morphological quantification of planula larvae**
244 After *Wnt3* knockdown by siRNA electroporation of *Clytia* or *Cladonema*, we
245 approximated the planula body shape into a two dimensional ellipse, measured both the
246 long and short axes (Figs. 4C and 6D), and calculated the aspect ratio of those values
247 using Fiji/ImageJ software (Figs 4D, 6E).
248
249
250 **RT-qPCR**
251 For *Clytia* and *Cladonema* samples, total RNA was extracted with RNeasy Mini or Micro
252 kits (Qiagen). Lysate was treated with DNaseI (Qiagen) for 15 min at room temperature
253 (RT). cDNA was synthesized with the PrimeScript II 1st strand synthesis kit (Takara bio).
254 RT-qPCR was performed with CFX connect (Bio-Rad) using iTaqTM universal SYBER

Green Supermix (Bio-Rad) or the QuantStudio 6 Flex Real-Time PCR System (Thermo Fisher) using TB Green Premix Ex TaqII (Tli RNaseH Plus) (Takara, RR820). Gene expressions were normalized to the housekeeping gene, *EF1alpha*, and the delta-delta-ct method was used for quantification (CFX maestro software, Bio-Rad or QuantStudio 6 Flex Real-Time PCR System software, Thermo Fisher).

For *Nematostella* samples, total RNA was extracted using the RNeasy Mini Kit and RNase-Free DNase Set (Qiagen). cDNA synthesis was conducted using the SuperScript IV First-Strand Synthesis System (Thermo Fisher). RT-qPCR was performed with the StepOnePlusTM Real-Time PCR System (Applied Biosystems, Thermo Fisher) using PowerUP SYBR Green Master Mix (Thermo Fisher). Gene expressions were normalized to the housekeeping gene, *NvEf1alpha*, and the delta-delta-ct method was used for quantification (StepOne™ and StepOnePlus™ Software v2.3).

Sequence alignment

Wnt3 amino acid sequence alignment was performed by ClustalW[46]. GenBank accession numbers and protein names are ABG49501.1 Wnt3 [*Xenopus tropicalis*], BAB70502.1 WNT3 [*Homo sapiens*], ABK90822.1 Wnt3 [*Gallus gallus*], ACB15465.1 Wnt3 [*Clytia hemisphaerica*], ABF48092.1 secreted signaling factor Wnt3, partial [*Nematostella vectensis*], CAK50826.1 Wnt3 protein precursor, partial [*Hydractinia echinata*], XP_015753662.1 PREDICTED: protein Wnt-3a-like isoform X2 [*Acropora digitifera*], XP_015753659.1 PREDICTED: protein Wnt-3a-like isoform X1 [*Acropora digitifera*], XP_032241388.1 protein Wnt-3a [*Nematostella vectensis*]. The alignment data was visualized and phylogenetic tree was constructed using neighbor joining and the BLOSUM62 matrix on Jalview software[47].

qPCR primers

Name	Sequence (5'->3')	
CpWnt3 qP FW	CAAATGTGGTCGATCAAACG	This study
CpWnt3 qP RV	TACGCCTTCTGCAACACTTG	This study
CpEF1-a_qPCR_F7	GGTCAATCTCGTTCCCTCCA	This study

CpEF1-a_qPCR_R7	TTTCCACCAGAGGTATCGGC	This study
CheGFP1 qP F	TTGCTGTCCGAATAGTGCAG	Fourrage et al., 2014 Open Biol
CheGFP1 qP RV	GACAACTCCTCCTCCGAGTG	Fourrage et al., 2014 Open Biol
CheWnt3 qP F	ATCATGGCAGGTGGAAACTC	Leclère et al., 2012 Dev Biol
CheWnt3 qP RV	CCCCATTTCCAACCTTCTTC	Leclère et al., 2012 Dev Biol
CheEF1a qP F	TGCTGTTGTCCCAATCTCTG	Leclère et al., 2012 Dev Biol / Fourrage et al., 2014 Open biol
CheEF1a qP RV	AAGACGGAGTGGTTTGGATG	Leclère et al., 2012 Dev Biol / Fourrage et al., 2014 Open biol
NvEf1alpha FW	GGTTGCCTCTTCGCTTACCACT	This strudy
NvEf1alpha RV	CGTTCCTGGCTTTAGGACAC	This study
NvBra1_Fw_1032	CGGGCTCACACTCTCACTTA	This study
NvBra1_Rv1174	CTTGCGGTATGGTGTTCCAG	This study

siRNA design

Name	Sequence (5'->3')		ORF
siCheGFP1_1 sense	CCAUCAGCUUCGAAAAUGAdTdT	This study	HQ397706.1
antisense	UCAUUUUCGAAGCUGAUGGdTdT	This study	
siCheGFP1_2 sense	UGAUGGCGCUUAUAAAGUUdTdT	This study	HQ397706.1
antisense	AACUUUAUAAGCGCCAUCAdTdT	This study	
siCheGFP1_3 sense	CGGACUCAUUCUUCAAAAAdTdT	This study	HQ397706.1
antisense	UUUUUGAAGAAUGAGUCCGdTdT	This study	
siCheWnt3_1 sense	GCAUGUGACUGUAAAUUUAdTdT	This study	EU374721.1
antisense	UAAAUUUACAGUCACAUGCdTdT	This study	
siCheWnt3_2 sense	ACAGCUUGGUAAAAUGUUAdTdT	This study	EU374721.1
antisense	UAACAUUUUACCAAGCUGUdTdT	This study	
siCpWnt3_1 sense	GUGGAACUGUAGUGUUUCAdTdT	This study	EU374721.1
antisense	UGAAACACUACAGUUCCACdTdT	This study	
siCpWnt3_2 sense	AGCGUGUGCUGAAGGUAAAdTdT	This study	EU374721.1
antisense	UUUACCUUCAGCACACGCUdTdT	This study	
siNvBra1_1 sense	GAAGAGAUCACGAGUCUAAdTdT	This study	AF540387.2
antisense	UUAGACUCGUGAUCUCUUCdTdT	This study	
siNegative_Control-1 for Nv sense	GCAACACGCAGAGTCGTAAdT	Same sequence as Karabulut et al, 2019 Dev Biol	
antisense	TTACGACTCTGCGTGTTGCdT	Same sequence as Karabulut et al, 2019 Dev Biol	

shRNA template

Name	Sequence (5'->3')	
CheWnt3_SI1_F	TAATACGACTCACTATA GCATGTGACTGTAAATTTA TTCAAGAGA TAAATTTACAGTCACATGC TT	This study

CheWnt3_SI1_R	AAGCATGTGACTGTAAATTTATCTCTTGAATAAATTTACAGTCACATGCTATAGTGAGTCGTATTA	This study
CheWnt3_SI2_F	TAATACGACTCACTATA ACAGCTTGGTAAAATGTTATTCAAGAGA TAACATTTTACCAAGCTGT TT	This study
CheWnt3_SI2_R	AAACAGCTTGGTAAAATGTTATCTCTTGAATAACATTTTACCAAGCTGTTATAGTGAGTCGTATTA	This study

290

291

292 ## Results

293

294 **Optimization of electroporation conditions**

295 In both hydrozoan jellyfish *Clytia hemisphaerica* and *Cladonema pacificum*,
296 gametogenesis is regulated by light-dark transitions[6,48]. A previous report showed that
297 *Clytia* medusae release eggs within 110-120 min or sperm within 60-90 min upon light
298 illumination after 3-8 h of darkness[12]. *Cladonema pacificum*, which live along coastal
299 areas in Japan, exhibit two types of gametogenesis depending on habitat: the dark-light
300 transition (light stimulation type) and the light-dark transition (dark stimulation type),
301 respectively. *Cladonema* medusae of the dark stimulation type, which we used in this
302 study, release eggs or sperm within 30 min upon dark stimulus after 20-24 h of constant
303 illumination[25,48]. By utilizing the characteristic gametogenesis of these jellyfish species,
304 we can control egg/sperm release and fertilization at any time of day. Indeed, we
305 routinely obtained *Clytia* sperm within 60 min and *Clytia* eggs within 90 min of light in a
306 13h dark/11h light cycle (Fig. 2A). Similarly, we collected gametes from *Cladonema*
307 within 25 min of dark stimulation in a 23.5h light/30 min dark cycle (Fig. 2A).

308 To determine optimal electroporation parameters, we first tested different
309 electroporation conditions and monitored the delivery efficiency of the red fluorescent
310 dye Rhodamine-Dextran into unfertilized *Clytia* and *Cladonema* eggs (Supplementary
311 Figs. 1-2). Given that the average molecular weight of siRNAs (21-mer, ~13,300 Da) are
312 similar to the molecular size of Rhodamine-Dextran (10,000 Da), electroporation trials
313 with Rhodamine-Dextran would visually confirm that small molecules are incorporated
314 into jellyfish eggs, as previously shown in *Hydractinia* eggs[38]. The collected eggs were
315 suspended in 15% Ficoll artificial seawater to prevent precipitation and to make a
316 homogeneous solution (Fig. 2B)[36,38]. We performed electroporation trails using
317 Rhodamine-Dextran using a cuvette with a 4 mm gap and tested several conditions of

318 voltage (V) and pulse length time (milliseconds, ms) using a conventional
319 electroporation system (Fig. 2C). As previous work showed that increasing the number
320 of pulses does not increase the Dextran delivery rate but decreases the survival rate of
321 embryos[38], we fixed the number of pulses to one and incubated unfertilized eggs with 1
322 mg/ml Dextrane-Rhodamine solution. *Clytia* eggs have little autofluorescence in the red
323 channel, and without electroporation (No EP), red fluorescence was rarely detected in
324 unfertilized eggs (Fig. 2D and Supplementary Fig. 1A). We compared the eight different
325 electroporation conditions and found that the rhodamine fluorescence was correlatively
326 detected in *Clytia* eggs depending on the strength of electric voltage, as long as the
327 voltage was in the range of 50-100 V（Supplementary Figs. 1B-1D）. By contrast, when
328 the voltage exceeded 200 V, the eggs were ruptured due to physical damage, and
329 cellular debris were observed（Supplementary Figs, 1E-1G）. We performed similar
330 electroporation trials on unfertilized *Cladonema* eggs with eight different conditions.
331 While red autofluorescence was negligible in the *Cladonema* eggs in the absence of
332 electroporation (Fig. 2D and Supplementary Fig. 2A), Rhodamine fluorescence was
333 frequently detected with 50 V (Fig. 2D and Supplementally Fig. 2E). In the more intense
334 conditions beyond 100 V (Supplementally Figs. 2F and 2G), the eggs were severely
335 damaged. Based on these results, we established the optimal electroporation condition
336 (50 V, 1 pulse, 25 ms) that allows high frequency of Dextran-positive eggs and low
337 levels of cell damage for both jellyfish eggs (Fig. 2D). Of note, during the initial trials, we
338 used unfertilized eggs, but we found that the electroporation process severely affected
339 the survival rate of embryos. In the case of *Cladonema*, electroporation before
340 fertilization severely decreased the survival rate of fertilized eggs (7.04% at 1 h post
341 fertilization) while electroporation after fertilization did not influence the survival rate (No
342 EP: 59.67%, With EP: 60.15%) (Supplementary Table 1). This dissimilarity is likely due
343 to the decrease of fertilization rate after electroporation, and both elapsed time after
344 spawning and physical damage by electroporation can affect fertilization efficiency.
345 Therefore, we decided to conduct further electroporation experiments with fertilized
346 eggs.
347
348
349 **Gene knockdown with siRNA in *Nematostella vectensis***

350 Before attempting gene knockdown via siRNAs electroporation in fertilized jellyfish
351 eggs, we first used *Nematostella vectensis,* where egg electroporation methodology has
352 been established[36]. We selected *Nematostella Brachyury* (*NvBra*), a gene expressed in
353 the blastopore margin that functions in the early embryo[49,50], as a target. After
354 electroporation of siRNAs targeting *NvBra* in fertilized eggs, we examined *NvBra*
355 expression in planula larvae at 3 days-post-fertilization (dpf) by RT-qPCR and found
356 that *NvBra* expression was drastically suppressed compared to no electroporation
357 controls and negative control siRNAs (Supplementary Fig. 3). We further evaluated
358 survival rates after electroporation and confirmed that siRNA electroporation does not
359 severely affect survival rates of 3 dpf planula at any of the tested conditions
360 (Supplementary Table 2). These results suggest that siRNA delivery into fertilized eggs
361 via electroporation is an effective gene knockdown method that is comparable to the
362 effect of shRNA delivery into unfertilized eggs via electroporation[36], supporting our
363 attempt to perform gene knockdown via siRNA electroporation using fertilized jellyfish
364 eggs.
365
366
367 **Endogenous *GFP1* knockdown with siRNA in *Clytia hemisphaerica***
368 The hydrozoan jellyfish *Clytia* endogenously expresses four green fluorescence proteins
369 (*CheGFP1-4*), and the distribution of each GFP expression dynamically changes across
370 its life cycle. For instance, *Clytia* eggs express maternal *CheGFP2* mRNA, and planula
371 larvae show typical ring-like *CheGFP1* fluorescence in the lateral ectoderm at 3 dpf[11].
372 While *CheGFP1* gene expression becomes dominant in the planula stage; *CheGFP2,*
373 *CheGFP3,* and *CheGFP4* are expressed in different tissues and organs in the
374 medusa[51]. Momose *et al*. succeeded in genome editing by injecting CRISPR/Cas9
375 targeting the endogenous *CheGFP1* into fertilized eggs, and confirmed the knockout
376 effect by loss of green fluorescence in 3 dpf planula larvae[11]. In addition, *CheGFP1* is
377 not essential for animal survival, which allows for the monitoring of knockdown effects
378 after embryogenesis. For these reasons, we chose endogenous *CheGFP1* for the first
379 target gene of siRNA knockdown.
380 In order to maximize the effect of gene knockdown, we used a combination of
381 three different siRNAs against *CheGFP1* in a mixture with a 1:1:1 ratio, and

382 electroporated 600 ng/μl of siRNA mix (200 ng/μl per each siRNA) into fertilized eggs
383 (Fig. 3A). To verify the effect of gene knockdown, we measured intensity of green
384 fluorescence of 2 dpf planula and found that siRNA (600ng/μl siRNA mix) electroporated
385 embryos showed dramatically reduced fluorescent intensity compared to the no-siRNA
386 controls (Figs. 3B-D; mean intensity value: 5.7×10^3 for 0 ng/μl control, 1.8×10^3 for 600
387 ng/μl). To evaluate the knockdown effects at varying doses of siRNA, we next
388 electroporated different concentrations of the *CheGFP1* siRNA mix (0, 150, 300, and
389 600 ng/μl) into fertilized eggs. While control 3 dpf planulae with no-electroporation (No
390 EP) as well as those with no-siRNA showed typical ring-shape GFP fluorescence in the
391 ectoderm, many planulae with *CheGFP1* siRNA electroporation lost green fluorescence
392 （Figs. 3E-3H）. To evaluate the GFP knockdown effects, we classified planulae with
393 typical GFP1 fluorescence as “wild type” and planulae with reduced fluorescence as
394 “reduced” for further quantification (Figs. 3I and 3J). The percentage of wild type
395 phenotype dramatically reduced in an siRNA dose-dependent manner (Fig. 3K). To
396 further quantify the above result at a molecular level, we examined relative *CheGFP1*
397 mRNA levels by RT-qPCR. Consistent with the image analysis results, we confirmed a
398 marked reduction of *CheGFP1* gene expression at different concentrations of *CheGFP1*
399 siRNA (Fig. 3L). These results demonstrate that siRNAs targeting *CheGFP1* repress its
400 expression upon electroporation and that the knockdown effects are dose-dependent.
401
402
403 ***Wnt3* knockdown with siRNA in *Clytia hemisphaerica***
404 Since electroporation of siRNAs targeting endogenous *CheGFP1* was shown to be
405 effective, we next decided to investigate the effects of knocking down other genes that
406 play important roles in early development. Wnt3 is a secreted signaling protein in the
407 Wnt/β-catenin pathway that is involved in diverse developmental processes including
408 cell fate decisions and patterning[52,53]. In *Clytia*, *Wnt3* RNA is maternally localized to the
409 animal cortex, the future oral side of the egg, and Wnt3 organizes axial patterning as
410 the main ligand for the Wnt/β-catenin pathway in the early embryonic stage[10]. After
411 embryogenesis, the *Clytia* planula normally elongates along the oral-aboral axis and
412 becomes oval in shape（Fig. 4A）. By contrast, after *CheWnt3* morpholino injection, the
413 morphant loses oral-aboral axis polarity and exhibits a spherical shape[10]. This raises the

414 possibility that knockdown of *CheWnt3* via siRNA may result in a similar spherical
415 morphology for *Clytia* larvae as observed in *CheWnt3* morphants. Therefore, to
416 evaluate siRNA knockdown effects on *Clytia*, we chose *CheWnt3* as our second target.
417 We used a mixture of two different siRNAs (1:1 ratio) targeting *CheWnt3*, and
418 carried out electroporation of the siRNA mix into *Clytia* fertilized eggs. After
419 electroporation of *CheWnt3* siRNAs, 1 dpf planula larvae showed nearly complete
420 spherical morphology (Fig. 4B), which is reminiscent of *CheWnt3* morphants[10]. To
421 quantify the effect of siRNA knockdown on *Clytia* larval morphology, we calculated the
422 aspect ratio in two dimensions, where values greater than 1.0 shows the tendency to be
423 oval (ellipsoid-like) while a value of 1.0 indicates a perfect circle (sphere) (Fig. 4C). The
424 control larvae with 0 ng/μl siRNA showed a median aspect ratio of 1.69, indicating a
425 typical ellipsoid-like morphology. By contrast, larvae that underwent electroporation with
426 *CheWnt3* siRNAs (400 ng/μl) showed a median aspect ratio of 1.16, suggesting a much
427 greater tendency toward spherical morphology (Fig. 4D). These results quantitively
428 confirmed the effect of *CheWnt*3 knockdown on larval morphology, which phenocopies
429 *CheWnt3* morphants[10]. To analyze the level of gene-specific knockdown at varying
430 doses of siRNAs, we next electroporated mixtures of 0, 100, 200, and 400 ng/μl of
431 *CheWnt3* siRNAs into *Clytia* fertilized eggs (Figs. 4E-4H). To evaluate *CheWnt3* siRNA
432 effects on morphology, we classified 1 dpf planulae with elongated ellipsoid-like shapes
433 as “normal” and planulae with spherical shapes as “spherical” (Figs. 4I and 4J). The
434 percentage of normal phenotype dramatically reduced after *CheWnt3* siRNA-
435 electroporation (< 1.0 % in 400 ng/μl), even at the lowest dose (5.2% in 100 ng/μl) (Fig.
436 4K). To further evaluate the result at a molecular level, we analyzed relative *CheWnt3*
437 mRNA levels by RT-qPCR and confirmed a significant reduction in *CheWnt3* gene
438 expression at all concentrations (Fig. 4L). Of note, after electroporation with universal
439 negative control siRNAs（Nippon gene co.Ltd）, both morphological phenotypes and
440 relative gene expression were comparable to no-siRNA controls (Supplementary Figs.
441 4A and 4B), further confirming that siRNA-mediated knockdown by electroporation is
442 target-specific. These results together indicate that siRNAs targeting endogenous genes
443 effectively knockdown their expression in *Clytia* embryos.
444
445

446 **Identification of *Wnt3* in *Cladonema pacificum***

447 In contrast to *Clytia*, the sole genetic model jellyfish, previous studies have neither
448 established genetic manipulation nor performed genome sequencing of *Cladonema*
449 *pacificum*, despite its unique biological features. This is partly because the extremely
450 small size of the *Cladonema* egg makes microinjection difficult. By testing whether
451 siRNA-mediated knockdown via electroporation can work in *Cladonema*, we can start to
452 manipulate genes in *Cladonema* while also demonstrating that siRNA electroporation
453 can be applicable to other jellyfish species. While green fluorescent protein (GFP) is
454 often an easy early target for gene manipulation in emerging organisms, *Cladonema*
455 does not exhibit apparent endogenous green fluorescence expression at any stage,
456 unlike *Clytia*. We instead turned our focus to *Wnt3* as the target for gene knockdown in
457 *Cladonema* since Wnt3 plays an important role in early embryonic development in
458 several cnidarian species[54,55].

459 To identify the *Wnt3* ortholog in *Cladonema*, we utilized the result of RNA-seq of
460 the *Cladonema* polyp, stolon, and medusa manubrium (data not shown). We performed
461 *Cladonema Wnt3* CDS annotation using *Clytia* CDS database (MARIMBA, Marine
462 models database: http://marimba.obs-vlfr.fr) and found one contig annotated with *Wnt3*
463 (*CpWnt3*). We then performed phylogenic analysis using the neighbor-joining method,
464 and confirmed *CpWnt3* (TRINITY_DN8032_c0_g1_i1.p1) is grouped with medusozoan
465 *Clytia Wnt3* rather than Anthozoa *Nematostella* and *Acropora digitifera* (Fig. 5A).
466 Multiple sequence alignment further showed highly conserved amino acids sequences
467 among different species including bilaterians and cnidarians (Fig. 5B). These findings
468 raise the possibility that *CpWnt3* has a similar function in controlling the Wnt/β-catenin
469 pathway in *Cladonema.*

470

471

472 ***Wnt3* knockdown with siRNA in *Cladonema pacificum***

473 Does *Wnt3* function during *Cladonema* embryogenesis, particularly during axial
474 patterning? Interestingly, *Cladonema* planula larvae do not show a clear elongated
475 shape (Fig. 6A), as observed in *Clytia*. It is thus possible that morphogenesis, including
476 axial patterning and/or the function of the Wnt/β-catenin pathway, differs between these
477 two jellyfish species.

In order to verify whether siRNA electroporation works in *Cladonema* and *Wnt3* affects axial patterning, we performed electroporation of siRNAs targeting *CpWnt3*. We prepared fertilized *Cladonema* eggs as we did in *Clytia*, and used a mixture of two different siRNAs against *CpWnt3* CDS with a 1:1 ratio (300 ng/μl) and performed electroporation with the previously established parameters (50V, 1 pulse, 25 ms) in fertilized *Cladonema* eggs. Strikingly, planula larvae after electroporation of siRNAs for *CpWnt3* did not exhibit morphological differences compared to controls（Figs. 6A-6C; median aspect ratio: 1.21 for 0 ng/μl control, 1.16 for 300 ng/μl for si*CpWnt3*）. We then quantified the morphological phenotypes by calculating the aspect ratio of 1 dpf planulae and confirmed that *CpWnt3* knockdown does not cause a significant morphological change (Figs. 6D and 6E). One possibility that would explain the above result is a defect in the siRNA knockdown itself. To test this potential explanation, we carried out RT-qPCR using mRNA samples from 1 dpf planula after electroporating different concentrations of *CpWnt3* siRNA mix (0, 150, and 300 ng/μl) into fertilized eggs. We confirmed a reduction of *Wnt3* gene expression in an siRNA dose-dependent manner (Fig. 6F), eliminating siRNA knockdown defects as the cause of our initial result. Taken together this work indicates that repression of *Wnt3* expression does not have a significant impact on *Cladonema* embryogenesis, at least on planula morphology. Given that overall oral-aboral polarity is less prominent in *Cladonema* compared to *Clytia*, the axial patterning mechanism may differ between these two jellyfish species.

Discussion

In this study, we have established a method to knock down endogenous genes in two hydrozoan jellyfish, *Clytia hemisphaerica* and *Cladonema pacificum*, via siRNA electroporation of fertilized eggs. We showed that knockdown of endogenous *GFP1* in *Clytia* causes the loss of GFP fluorescence in the planula stage, as previously achieved by CRISPR/Cas9-mediated *GFP1* knockout[11]. We also confirmed that knockdown of *Wnt3* in *Clytia* induces spherical morphology of the planula, mirroring the results of injections of *Wnt3* morpholino antisense oligo[10]. By contrast, although we succeeded in efficient repression of *Wnt3* gene expression in *Cladonema* after *Wnt3* siRNA

510 electroporation, the morphological phenotypes did not appear as observed in *Clytia*,
511 suggesting that the mechanism involved in embryogenesis and planula morphogenesis
512 may differ across hydrozoan jellyfish species.
513 Effective gene knockdown via shRNA electroporation has previously been
514 reported using two cnidarian polyps, *Nematostella vectensis* and *Hydractinia*
515 *symbiolongicarpus*[36,38]. We tested whether shRNAs are also effective in the hydrozoan
516 jellyfish *Clytia*. We designed shRNAs targeting *CheWnt3* using the same 19 bp target
517 sequence that was used for siRNAs, and performed electroporation on fertilized eggs
518 with a mix of two different *Wnt3* shRNAs. After electroporation of *Wnt3* shRNAs, relative
519 *Wnt3* mRNA expression in 1 dpf planula was weakly down-regulated (0.83), and was
520 not significant compared to the striking effects of *Wnt3* siRNA electroporation (0.039) at
521 the same concentration (400 ng/μl) (Supplementary Fig. 4A). In addition, electroporation
522 of *Wnt3* siRNAs resulted in severe morphological changes manifested by a spherical
523 shape, showing almost no "normal" phenotype (0.71%), whereas electroporation of
524 shRNA had a limited effect (60.4%) (Supplementary Fig. 4B). These results suggest
525 that the effect of siRNA is much stronger than that of shRNA in *Clytia* when treated with
526 the same target sequence and concentration.
527 One possibility that would explain such distinct effects between siRNA and
528 shRNA electroporation is the existence of differences in the RNAi machinery or
529 efficiency of RNA processing among cnidarians. During RNAi in mammals, the RNase
530 III Dicer protein processes shRNA in collaboration with cofactors TRBP (Transactivation
531 response element RNA-binding protein) and PACT（protein activator of the interferon-
532 induced protein kinase）to produce a mature form of siRNA[39]. Mature siRNA in the Dicer
533 and TRBP/PACT complex is associated with Argonaute protein and cleaves
534 endogenous complementary mRNAs as the RNA-induced silencing complex [30,56].
535 These small RNA biogenesis factors, Dicers and cofactors (TRBP in bilaterians, HYL1
536 in plants and cnidarians), are found in *Nematostella vectensis*, *Acropora digitifera*, and
537 *Hydra vulgaris*[41]. Although Dicers (TCONS_00004571 and TCONS_00004525) and
538 Hyl1 (TCONS_00010722) are predicted to exist in *Clytia* from the MARIMBA
539 transcriptome data, the expression level of Dicers in oocytes and early gastrulation
540 stages is lower than that in other stages, suggesting the possibility that insufficient
541 efficiency of shRNA to siRNA processing is responsible for the difference in knockdown

542 efficiency between siRNA and shRNA electroporation. It will be interesting to elucidate
543 the detailed molecular mechanism of RNAi in different cnidarian species and address
544 RNA processing efficiency in distinct developmental stages.
545 During *Clytia* early embryogenesis, *Wnt3* RNA is localized to the animal cortex of
546 the egg and contributes to the formation of the oral-aboral axis[10]. Accordingly,
547 knockdown of *Wnt3* in *Clytia* fertilized eggs induces suppression of axis formation and
548 planula elongation (Fig. 4). In contrast, no morphological phenotype was observed after
549 *Wnt3* knockdown in *Cladonema*, despite a marked decrease in its gene expression (Fig.
550 6). This result was in stark contrast to the *Wnt3* loss-of-function phenotypes in *Clytia.*
551 We thought the divergence in outcome may be due to large differences in *Cladonema*
552 and *Clytia Wnt3*, but amino acid alignment results demonstrate that *Cladonema Wnt3* is
553 homologous to *Wnt3* in other cnidarians and is highly homologous to *Clytia Wnt3* (Fig.
554 5B). Beyond *Clytia*, the Wnt/β-catenin signaling pathway is involved in axis formation in
555 *Nematostella*[54,57]. Furthermore, given the similar localization of the Wnt ligand in
556 *Hydractinia*[55,58], the Wnt/β-catenin pathway likely functions in early *Cladonema*
557 development to some extent. One possibility that accounts for the morphological
558 phenotype of *Wnt3* knockdown in *Cladonema* is that several Wnt ligands act
559 redundantly. Indeed, we found multiple *Wnt* genes in *Cladonema* from transcriptome
560 data (Supplementary Fig. 5). Another possibility is that the limited elongation in
561 *Cladonema* planulae might hamper phenotypical appearance upon inhibition of Wnt/β-
562 catenin signaling. Understanding the diversity and differences of gastrulation and
563 planula morphogenesis in cnidarians is an interesting and unresolved topic for future
564 studies.
565 An interesting feature of jellyfish is that their morphology dramatically changes
566 across their life cycle from planula to polyp and then to medusa. In particular, polyps
567 and medusae, different adult stages of the same animal, exhibit distinct regenerative
568 ability, lifespan, and behaviors. Although regeneration mechanisms have been
569 extensively studied in polyp-only animals such as *Hydra* and *Hydractinia*, classical
570 studies have used the medusa stage of several jellyfish species and demonstrated their
571 regenerative potential[21]. Recent work using *Clytia* medusae has further shown a
572 remarkable remodeling and repatterning mechanism orchestrated by muscle systems
573 upon organ loss[17]. At the behavior level, the upside-down jellyfish *Cassiopea* medusae

574 exhibit a sleep-like state[59], which is similarly observed in *Hydra* polyps[60]. More recent
575 work using transgenic *Clytia* has characterized feeding behaviors in medusae at a
576 neural-network resolution[19]. To understand how these diverse biological processes in
577 jellyfish are regulated at the molecular level, it is necessary to analyze the functions of
578 specific genes at various stages. Although gene knockdown by dsRNA electroporation
579 into polyps in the scyphozoan jellyfish *Aurelia* had been reported[61], genetic
580 manipulation in medusae has not yet been achieved. Given that siRNA electroporation
581 is applicable to *Hydra* polyps[33,62] in addition to cnidarian fertilized eggs, we now have a
582 better chance to apply this technique to the medusa stage by adjusting established
583 conditions. Our method of gene knockdown via siRNA electroporation will complement
584 the method of shRNA electroporation in cnidarian polyps and promise molecular-level
585 analysis of interesting biological phenomena associated with different life stages in
586 jellyfish.
587
588
589 **References**

590 1 Technau, U. & Steele, R. E. Evolutionary crossroads in developmental biology:
591 Cnidaria. *Development* **138**, 1447-1458, doi:10.1242/dev.048959 (2011).
592 2 Zapata, F. *et al.* Phylogenomic Analyses Support Traditional Relationships within
593 Cnidaria. *PLoS One* **10**, e0139068, doi:10.1371/journal.pone.0139068 (2015).
594 3 Leclere, L. & Rottinger, E. Diversity of Cnidarian Muscles: Function, Anatomy,
595 Development and Regeneration. *Front Cell Dev Biol* **4**, 157,
596 doi:10.3389/fcell.2016.00157 (2016).
597 4 Holstein, T. W., Hobmayer, E. & Technau, U. Cnidarians: an evolutionarily
598 conserved model system for regeneration? *Dev Dyn* **226**, 257-267,
599 doi:10.1002/dvdy.10227 (2003).
600 5 Bosch, T. C. G. *et al.* Back to the Basics: Cnidarians Start to Fire. *Trends*
601 *Neurosci* **40**, 92-105, doi:10.1016/j.tins.2016.11.005 (2017).
602 6 Houliston, E., Momose, T. & Manuel, M. Clytia hemisphaerica: a jellyfish cousin
603 joins the laboratory. *Trends Genet* **26**, 159-167, doi:10.1016/j.tig.2010.01.008
604 (2010).

605 7 Houliston, E., Leclere, L., Munro, C., Copley, R. R. & Momose, T. Past, present
606 and future of Clytia hemisphaerica as a laboratory jellyfish. *Curr Top Dev Biol*,
607 doi:10.1016/bs.ctdb.2021.12.014 (2022).
608 8 Lechable, M. *et al.* An improved whole life cycle culture protocol for the
609 hydrozoan genetic model Clytia hemisphaerica. *Biol Open* **9**,
610 doi:10.1242/bio.051268 (2020).
611 9 Momose, T. & Houliston, E. Two oppositely localised frizzled RNAs as axis
612 determinants in a cnidarian embryo. *PLoS Biol* **5**, e70,
613 doi:10.1371/journal.pbio.0050070 (2007).
614 10 Momose, T., Derelle, R. & Houliston, E. A maternally localised Wnt ligand
615 required for axial patterning in the cnidarian Clytia hemisphaerica. *Development*
616 **135**, 2105-2113, doi:10.1242/dev.021543 (2008).
617 11 Momose, T. *et al.* High doses of CRISPR/Cas9 ribonucleoprotein efficiently
618 induce gene knockout with low mosaicism in the hydrozoan Clytia hemisphaerica
619 through microhomology-mediated deletion. *Sci Rep* **8**, 11734,
620 doi:10.1038/s41598-018-30188-0 (2018).
621 12 Quiroga Artigas, G. *et al.* A gonad-expressed opsin mediates light-induced
622 spawning in the jellyfish Clytia. *Elife* **7**, doi:10.7554/eLife.29555 (2018).
623 13 Quiroga Artigas, G. *et al.* A G protein-coupled receptor mediates neuropeptide-
624 induced oocyte maturation in the jellyfish Clytia. *PLoS Biol* **18**, e3000614,
625 doi:10.1371/journal.pbio.3000614 (2020).
626 14 Lapebie, P. *et al.* Differential responses to Wnt and PCP disruption predict
627 expression and developmental function of conserved and novel genes in a
628 cnidarian. *PLoS Genet* **10**, e1004590, doi:10.1371/journal.pgen.1004590 (2014).
629 15 Condamine, T. *et al.* Molecular characterisation of a cellular conveyor belt in
630 Clytia medusae. *Dev Biol* **456**, 212-225, doi:10.1016/j.ydbio.2019.09.001 (2019).
631 16 Leclere, L. *et al.* The genome of the jellyfish Clytia hemisphaerica and the
632 evolution of the cnidarian life-cycle. *Nat Ecol Evol* **3**, 801-810,
633 doi:10.1038/s41559-019-0833-2 (2019).
634 17 Sinigaglia, C. *et al.* Pattern regulation in a regenerating jellyfish. *Elife* **9**,
635 doi:10.7554/eLife.54868 (2020).

636 18 Chari, T. *et al.* Whole-animal multiplexed single-cell RNA-seq reveals
637 transcriptional shifts across Clytia medusa cell types. *Sci Adv* **7**, eabh1683,
638 doi:10.1126/sciadv.abh1683 (2021).
639 19 Weissbourd, B. *et al.* A genetically tractable jellyfish model for systems and
640 evolutionary neuroscience. *Cell* **184**, 5854-5868 e5820,
641 doi:10.1016/j.cell.2021.10.021 (2021).
642 20 Leclere, L. *et al.* Maternally localized germ plasm mRNAs and germ cell/stem cell
643 formation in the cnidarian Clytia. *Dev Biol* **364**, 236-248,
644 doi:10.1016/j.ydbio.2012.01.018 (2012).
645 21 Fujita, S., Kuranaga, E. & Nakajima, Y. I. Regeneration Potential of Jellyfish:
646 Cellular Mechanisms and Molecular Insights. *Genes (Basel)* **12**,
647 doi:10.3390/genes12050758 (2021).
648 22 Fujiki, A., Hou, S., Nakamoto, A. & Kumano, G. Branching pattern and
649 morphogenesis of medusa tentacles in the jellyfish Cladonema pacificum
650 (Hydrozoa, Cnidaria). *Zoological Lett* **5**, 12, doi:10.1186/s40851-019-0124-4
651 (2019).
652 23 Fujita, S., Kuranaga, E. & Nakajima, Y. I. Cell proliferation controls body size
653 growth, tentacle morphogenesis, and regeneration in hydrozoan jellyfish
654 Cladonema pacificum. *PeerJ* **7**, e7579, doi:10.7717/peerj.7579 (2019).
655 24 Hou, S., Zhu, J., Shibata, S., Nakamoto, A. & Kumano, G. Repetitive
656 accumulation of interstitial cells generates the branched structure of Cladonema
657 medusa tentacles. *Development* **148**, doi:10.1242/dev.199544 (2021).
658 25 Takeda, N. *et al.* Identification of jellyfish neuropeptides that act directly as
659 oocyte maturation-inducing hormones. *Development* **145**,
660 doi:10.1242/dev.156786 (2018).
661 26 Stierwald, M., Yanze, N., Bamert, R. P., Kammermeier, L. & Schmid, V. The Sine
662 oculis/Six class family of homeobox genes in jellyfish with and without eyes:
663 development and eye regeneration. *Dev Biol* **274**, 70-81,
664 doi:10.1016/j.ydbio.2004.06.018 (2004).
665 27 Suga, H., Schmid, V. & Gehring, W. J. Evolution and functional diversity of
666 jellyfish opsins. *Curr Biol* **18**, 51-55, doi:10.1016/j.cub.2007.11.059 (2008).

667 28 Suga, H. *et al.* Flexibly deployed Pax genes in eye development at the early
668 evolution of animals demonstrated by studies on a hydrozoan jellyfish. *Proc Natl*
669 *Acad Sci U S A* **107**, 14263-14268, doi:10.1073/pnas.1008389107 (2010).
670 29 Graziussi, D. F., Suga, H., Schmid, V. & Gehring, W. J. The "eyes absent" (eya)
671 gene in the eye-bearing hydrozoan jellyfish Cladonema radiatum: conservation of
672 the retinal determination network. *J Exp Zool B Mol Dev Evol* **318**, 257-267,
673 doi:10.1002/jez.b.22442 (2012).
674 30 Meister, G. & Tuschl, T. Mechanisms of gene silencing by double-stranded RNA.
675 *Nature* **431**, 343-349, doi:10.1038/nature02873 (2004).
676 31 Rao, D. D., Vorhies, J. S., Senzer, N. & Nemunaitis, J. siRNA vs. shRNA:
677 similarities and differences. *Adv Drug Deliv Rev* **61**, 746-759,
678 doi:10.1016/j.addr.2009.04.004 (2009).
679 32 Moran, Y. *et al.* Cnidarian microRNAs frequently regulate targets by cleavage.
680 *Genome Res* **24**, 651-663, doi:10.1101/gr.162503.113 (2014).
681 33 Watanabe, H. *et al.* Nodal signalling determines biradial asymmetry in Hydra.
682 *Nature* **515**, 112-115, doi:10.1038/nature13666 (2014).
683 34 Pankow, S. & Bamberger, C. The p53 tumor suppressor-like protein nvp63
684 mediates selective germ cell death in the sea anemone Nematostella vectensis.
685 *PLoS One* **2**, e782, doi:10.1371/journal.pone.0000782 (2007).
686 35 He, S. *et al.* An axial Hox code controls tissue segmentation and body patterning
687 in Nematostella vectensis. *Science* **361**, 1377-1380,
688 doi:10.1126/science.aar8384 (2018).
689 36 Karabulut, A., He, S., Chen, C. Y., McKinney, S. A. & Gibson, M. C.
690 Electroporation of short hairpin RNAs for rapid and efficient gene knockdown in
691 the starlet sea anemone, Nematostella vectensis. *Dev Biol* **448**, 7-15,
692 doi:10.1016/j.ydbio.2019.01.005 (2019).
693 37 DuBuc, T. Q. *et al.* Transcription factor AP2 controls cnidarian germ cell
694 induction. *Science* **367**, 757-762, doi:10.1126/science.aay6782 (2020).
695 38 Quiroga-Artigas, G., Duscher, A., Lundquist, K., Waletich, J. & Schnitzler, C. E.
696 Gene knockdown via electroporation of short hairpin RNAs in embryos of the
697 marine hydroid Hydractinia symbiolongicarpus. *Sci Rep* **10**, 12806,
698 doi:10.1038/s41598-020-69489-8 (2020).

699 39 Ha, M. & Kim, V. N. Regulation of microRNA biogenesis. *Nat Rev Mol Cell Biol*
700 **15**, 509-524, doi:10.1038/nrm3838 (2014).
701 40 Krishna, S. *et al.* Deep sequencing reveals unique small RNA repertoire that is
702 regulated during head regeneration in Hydra magnipapillata. *Nucleic Acids Res*
703 **41**, 599-616, doi:10.1093/nar/gks1020 (2013).
704 41 Moran, Y., Praher, D., Fredman, D. & Technau, U. The evolution of microRNA
705 pathway protein components in Cnidaria. *Mol Biol Evol* **30**, 2541-2552,
706 doi:10.1093/molbev/mst159 (2013).
707 42 Murchison, E. P., Partridge, J. F., Tam, O. H., Cheloufi, S. & Hannon, G. J.
708 Characterization of Dicer-deficient murine embryonic stem cells. *Proc Natl Acad*
709 *Sci U S A* **102**, 12135-12140, doi:10.1073/pnas.0505479102 (2005).
710 43 Kok, K. H., Ng, M. H., Ching, Y. P. & Jin, D. Y. Human TRBP and PACT directly
711 interact with each other and associate with dicer to facilitate the production of
712 small interfering RNA. *J Biol Chem* **282**, 17649-17657,
713 doi:10.1074/jbc.M611768200 (2007).
714 44 Watanabe, H. *et al.* Sequential actions of beta-catenin and Bmp pattern the oral
715 nerve net in Nematostella vectensis. *Nat Commun* **5**, 5536,
716 doi:10.1038/ncomms6536 (2014).
717 45 Schindelin, J. *et al.* Fiji: an open-source platform for biological-image analysis.
718 *Nat Methods* **9**, 676-682, doi:10.1038/nmeth.2019 (2012).
719 46 Thompson, J. D., Higgins, D. G. & Gibson, T. J. CLUSTAL W: improving the
720 sensitivity of progressive multiple sequence alignment through sequence
721 weighting, position-specific gap penalties and weight matrix choice. *Nucleic Acids*
722 *Res* **22**, 4673-4680, doi:10.1093/nar/22.22.4673 (1994).
723 47 Waterhouse, A. M., Procter, J. B., Martin, D. M., Clamp, M. & Barton, G. J.
724 Jalview Version 2--a multiple sequence alignment editor and analysis workbench.
725 *Bioinformatics* **25**, 1189-1191, doi:10.1093/bioinformatics/btp033 (2009).
726 48 Deguchi, R., Kondoh, E. & Itoh, J. Spatiotemporal characteristics and
727 mechanisms of intracellular Ca(2+) increases at fertilization in eggs of jellyfish
728 (Phylum Cnidaria, Class Hydrozoa). *Dev Biol* **279**, 291-307,
729 doi:10.1016/j.ydbio.2004.11.036 (2005).

730 49 Scholz, C. B. & Technau, U. The ancestral role of Brachyury: expression of
731 NemBra1 in the basal cnidarian Nematostella vectensis (Anthozoa). *Dev Genes*
732 *Evol* **212**, 563-570, doi:10.1007/s00427-002-0272-x (2003).
733 50 Servetnick, M. D. *et al.* Cas9-mediated excision of Nematostella brachyury
734 disrupts endoderm development, pharynx formation and oral-aboral patterning.
735 *Development* **144**, 2951-2960, doi:10.1242/dev.145839 (2017).
736 51 Fourrage, C., Swann, K., Gonzalez Garcia, J. R., Campbell, A. K. & Houliston, E.
737 An endogenous green fluorescent protein-photoprotein pair in Clytia
738 hemisphaerica eggs shows co-targeting to mitochondria and efficient
739 bioluminescence energy transfer. *Open Biol* **4**, 130206, doi:10.1098/rsob.130206
740 (2014).
741 52 Guder, C. *et al.* The Wnt code: cnidarians signal the way. *Oncogene* **25**, 7450-
742 7460, doi:10.1038/sj.onc.1210052 (2006).
743 53 Lee, P. N., Pang, K., Matus, D. Q. & Martindale, M. Q. A WNT of things to come:
744 evolution of Wnt signaling and polarity in cnidarians. *Semin Cell Dev Biol* **17**,
745 157-167, doi:10.1016/j.semcdb.2006.05.002 (2006).
746 54 Kraus, Y., Aman, A., Technau, U. & Genikhovich, G. Pre-bilaterian origin of the
747 blastoporal axial organizer. *Nat Commun* **7**, 11694, doi:10.1038/ncomms11694
748 (2016).
749 55 Plickert, G., Jacoby, V., Frank, U., Muller, W. A. & Mokady, O. Wnt signaling in
750 hydroid development: formation of the primary body axis in embryogenesis and
751 its subsequent patterning. *Dev Biol* **298**, 368-378,
752 doi:10.1016/j.ydbio.2006.06.043 (2006).
753 56 Bartel, D. P. MicroRNAs: genomics, biogenesis, mechanism, and function. *Cell*
754 **116**, 281-297, doi:10.1016/s0092-8674(04)00045-5 (2004).
755 57 DuBuc, T. Q., Stephenson, T. B., Rock, A. Q. & Martindale, M. Q. Hox and Wnt
756 pattern the primary body axis of an anthozoan cnidarian before gastrulation. *Nat*
757 *Commun* **9**, 2007, doi:10.1038/s41467-018-04184-x (2018).
758 58 Duffy, D. J., Plickert, G., Kuenzel, T., Tilmann, W. & Frank, U. Wnt signaling
759 promotes oral but suppresses aboral structures in Hydractinia metamorphosis
760 and regeneration. *Development* **137**, 3057-3066, doi:10.1242/dev.046631
761 (2010).

59 Nath, R. D. *et al.* The Jellyfish Cassiopea Exhibits a Sleep-like State. *Curr Biol* **27**, 2984-2990 e2983, doi:10.1016/j.cub.2017.08.014 (2017).
60 Kanaya, H. J. *et al.* A sleep-like state in Hydra unravels conserved sleep mechanisms during the evolutionary development of the central nervous system. *Sci Adv* **6**, doi:10.1126/sciadv.abb9415 (2020).
61 Fuchs, B. *et al.* Regulation of polyp-to-jellyfish transition in Aurelia aurita. *Curr Biol* **24**, 263-273, doi:10.1016/j.cub.2013.12.003 (2014).
62 Lommel, M. *et al.* Hydra Mesoglea Proteome Identifies Thrombospondin as a Conserved Component Active in Head Organizer Restriction. *Sci Rep* **8**, 11753, doi:10.1038/s41598-018-30035-2 (2018).

Acknowledgement

We thank R. Deguchi (Miyagi Univ. Education, Japan) for sharing *Cladonema pacificum* and EMBRC France for sharing *Clytia hemisphaerica*. We thank T. Momose (Sorbonne University, CNRS, France) for helpful discussion. We thank I. Nagai and A. Sasaki for technical assistance; and A. Dahal, A. Tanimoto, and J. Higuchi for *Nematostella* culture. This work was supported by JST grant number JPMJCR1852 to E.K., AMED under grant number JP21gm6110025 to Y.N., and the JSPS KAKENHI grant numbers 21H05255 to E.K., and JP17H06332 and JP19K22550 to Y.N.

Author contributions

T.M.-O. conceptualized and designed the project, performed experiments using jellyfish, analyzed data, prepared figures, and wrote the manuscript. S.F. performed experiments and analyzed data. R.N. performed experiments using *Nematostella*. H.W. conceptualized and designed the project. E.K. contributed to reagents. Y.N. conceptualized and designed the project, prepared figures, and wrote the manuscript. All authors approved the final manuscript.

Competing interests

794 The authors declare no competing interests.
795
796
797 ## Figure legends
798
799 **Figure 1. The hydrozoan jellyfish *Clytia hemisphaerica* and *Cladonema pacificum*.**
800 (**A**) The cladogram depicting the phylogenetic position of cnidarian jellyfish. As the sister
801 group of Bilateria, the phylum Cnidaria is divided into two clades, Anthozoa and
802 Medusozoa, which consists of four classes: Hydrozoa, Staurozoa, Scyphozoa, and
803 Cubozoa. Hydorozoa includes polyp type animals without a medusa stage (e.g. *Hydra*
804 and *Hydractinia*) and jellyfish that have both polyp and medusa stages (e.g. *Clytia* and
805 *Cladonema*). (**B** and **C**) Photos of an adult medusa and eggs of *Clytia hemisphaerica*
806 (**B**) and *Cladonema pacificum* (**C**). Scale bars: 1 mm for medusae; 100 μm for eggs.
807
808
809 **Figure 2. The electroporation procedure for jellyfish eggs.** (**A**) Schematic of
810 spawning under the 24 h light/dark cycle. *Clytia hemisphaerica* are maintained in a 13 h
811 dark/11 h light cycle. After light stimuli, sperm spawning occurs within 60-90 min and
812 egg spawning occurs within 90-120 min. *Cladonema pacificum* are maintained in a 23.5
813 h light/0.5 h dark cycle. After dark stimuli, sperm and egg spawning occurs within 25
814 min. (**B**) Fertilized eggs are resuspended in 15% Ficoll/artificial sea water to prevent
815 precipitation of eggs during electroporation. (**C**) Electroporation is performed with the
816 Bio-Rad Gene Pulser Xcell electroporation system and a cuvette with a 4 mm gap. (**D**)
817 Visualization of the Rhodamine-Dextran delivery into eggs by electroporation.
818 Rhodamine is shown in red. While little or no fluorescence was observed in eggs
819 without electroporation (No EP), under the condition of a single 50 V pulse for 25 ms,
820 rhodamine signals were detected in both *Clytia and Cladonema* eggs without cell
821 damage. For clarity, egg outlines are indicated with dashed lines for eggs without
822 electroporation. Scale bars: 200 μm.
823
824

825 **Figure 3**. **Phenotypes of *GFP1* knockdown with siRNA in *Clytia* fertilized eggs.** (**A**)
826 Schematic of the siRNA electroporation procedure using fertilized eggs. Fertilized eggs
827 in 15% Ficoll/artificial sea water mixed with siRNA are incubated for 5 min, and
828 electroporation is conducted after transferring into a cuvette. (**B** and **C**) Phenotypes of
829 *Clytia* 2-day planula after *CheGFP1* siRNA knockdown. (**D**) Boxplots showing the GFP
830 fluorescence intensity mean values in 2-day planula after electroporation of 0 and 600
831 ng/μl siRNAs targeting *CheGFP1*. Center lines indicate the medians; x's denote the
832 means; box limits represent the 25th and 75th percentiles; whiskers show the maximum
833 and minimum values. (**E**-**H**) Phenotypes of 3-day planula after siRNA targeting
834 *CheGFP1* electroporation (0, 150, 300, and 600 ng/μl si*CheGFP1*). (**I** and **J**) For
835 quantification of green fluorescence, we classified phenotypes into two categories:
836 planula with ring-like green fluorescence as "wild-type," and planula with reduced green
837 fluorescence as "reduced". (**K**) Quantification of planula larvae positive for *CheGFP1*
838 (wild-type). Bar plots show the percentage of wild-type phenotype after *CheGFP1*
839 knockdown. Number of examined planula: 0 ng/μl, *n*=82; 150 ng/μl, *n*=64; 300 ng/μl,
840 *n*=58; 600 ng/μl, *n*=114. Error bars: maximum and minimum values. (**L**) Quantification of
841 *CheGFP1* mRNA expression levels in 3-day planula by RT-qPCR. *CheEF1a* was used
842 as an internal control. Bar heights represent mean values of at least three independent
843 experiments. *CheGFP1* expression levels are standardized relative to the control (0
844 ng/μl) condition. Error bars: standard deviation. Scale bars: 200 μm.
845
846
847 **Figure 4. Phenotypes of *Wnt3* knockdown with siRNA in *Clytia* fertilized eggs.** (**A**
848 and **B**) Typical phenotypes of *Clytia* 1-day planula. While morphologies of control
849 planula (0 ng/μl) have an elongated oval-shape (A), those of *CheWnt3* siRNA (400
850 ng/μl) are spherical in shape (**B**). (**C**) Schematic of ellipse approximation for planula
851 morphology and calculation of the aspect ratio. The aspect ratio was calculated by
852 dividing the long axis (a) by short axis (b). (**D**) Boxplots showing the aspect ratio of the
853 1-day planula. Center lines show the medians; x's denote the mean values; box limits
854 indicate the 25th and 75th percentiles; whiskers show maximum and minimum values;
855 inner points and outliers are represented by circles. Number of examined planula: 0
856 ng/μl, *n*=127; 400 ng/μl, *n*=25. (**E**-**H**) Phenotypes of 1-day planula after siRNA targeting

857 *CheWnt3* electroporation (0, 100, 200, and 400 ng/μl si*CheWnt3*). (**I** and **J**) For
858 morphology quantification, we classified planula phenotypes into two categories:
859 elongated oval shape as "normal" and spherical (circle) shape as "spherical". (**K**) Bar
860 plots show the percentage of normal phenotypes across four different siRNA doses.
861 Percentages are the mean value of three independent experiments, and error bars
862 indicate standard deviation. Numbers of examined planula: 0 ng/μl, *n*=127; 100 ng/μl,
863 *n*=75; 200 ng/μl, *n*=86; 400 ng/μl, *n*=95. Error bars: maximum and minimum values. (**L**)
864 Quantification of *CheWnt3* mRNA levels of 1-day planula by RT-qPCR. *CheEF1a* was
865 used as an internal control. Bar heights represent the mean value of at least three
866 independent experiments. *CheWnt3* expression levels are standardized relative to the
867 control (0 ng/μl). Error bars: standard deviation. Scale bars: (A, B, E-H) 400 μm, (I, J)
868 100 μm.
869
870
871 **Figure 5. Identification of *Cladonema Wnt3* by phylogenetic analyses.** (**A**) The
872 results of (**A**) phylogenetic analyses and (**B**) sequence alignment of Wnt3 among
873 indicated species. Amino acid sequence alignment was performed with ClustalW.
874 Alignment visualization and phylogenetic tree calculation were done with the Jalview
875 software. Cnidarian Wnt3 proteins are highlighted in blue and *Cladonema* Wnt3 is
876 highlighted in red. In sequence alignment, consensus residues are colored. Wnt3
877 proteins are universally conserved among animals. *He, Hydractinia echinate; Cp,*
878 *Cladonema pacificum; Che, Clytia hemisphaerica; Nv, Nematostella vectensis; Ad,*
879 *Acropora digitifera; Hs, Homo sapiens; Gg, Gallus gallus; Xt, Xenopus tropicalis.*
880 GenBank accession numbers are shown in "Materials and methods."
881
882
883 **Figure 6. Phenotypes of *Wnt3* knockdown with siRNA and Wnt/β-catenin pathway**
884 **inhibitor treatment in *Cladonema* fertilized eggs.** (**A**) Typical morphology of
885 *Cladonema* egg and planula. The wild-type *Cladonema* planula larvae exhibit a short
886 oval shape. To deliver siRNAs targeting *CpWnt3,* electroporation was performed in
887 fertilized eggs (1-cell stage), and phenotypes were confirmed at planula in one day. (**B**
888 and **C**) Phenotypes of 1-day planula after *CpWnt3* siRNA knockdown. (**D**) Schematic of

889 ellipse approximation for planula morphology and calculation of the aspect ratio. The
890 aspect ratio was calculated by dividing the long axis (a) by short axis (b). (**E**) Boxplots
891 showing the aspect ratio of the 1-day planula after si*CpWnt3* electroporation (0 and 300
892 ng/μl). Center lines show the medians; x's denote the mean values; box limits indicate
893 the 25th and 75th percentiles; whiskers show maximum and minimum values; inner
894 points and outliers are represented by circles. Number of examined planulae: 0 ng/μl,
895 *n*=22; 300 ng/μl, *n*=50. (**F**) Quantification of *CpWnt3* mRNA levels in 1-day planula by
896 RT-qPCR. *CpEF1a* was used as an internal control. Bar heights represent the mean
897 value of at least three independent experiments. Error bars indicate standard deviation.
898 *CpWnt3* expression levels are standardized relative to the control (0 ng/μl). Scale bars:
899 (B, C) 200μm.
900
901
902 ## Supplementary materials
903
904 **Supplementary Figure 1. Dextran delivery to *Clytia* eggs under different**
905 **electroporation conditions.** (**A**-**G**) Photos of unfertilized *Clytia* eggs after
906 electroporation of Dextran-Rhodamine (1 mg/ml) in indicated conditions. Fluorescence
907 intensity tends to increase in a voltage and time dependent manner. In the severe
908 conditions above 200 V (**E**-**G**), eggs were severely damaged. Scale bars: 200 μm.
909
910
911 **Supplementary Figure 2. Dextran delivery to *Cladonema* eggs under different**
912 **electroporation conditions.** (**A**-**F**) Photos of unfertilized *Cladonema* eggs after
913 electroporation of Dextran-Rhodamine (1 mg/ml) in indicated conditions. Fluorescence
914 was frequently detected beyond 50 V, but in the severe conditions (**E** and **F**), eggs were
915 severely damaged. Scale bars: 200 μm.
916
917
918 **Supplementary Figure 3. Gene knockdown with siRNA via electroporation into**
919 ***Nematostella* fertilized eggs.** qPCR quantification of *Nematostella Brachyury* (*NvBra*)
920 mRNA expression in siRNA-electroporated planulae (3 dpf). *NvEf1alpha* was used as

921 the internal control. Shown are the results of the mean ± S.D. from a single experiment
922 in triplicate, representing at least two independent experiments with similar results.
923
924
925 **Supplementary Figure 4. Comparison of siRNA and shRNA in *Clytia.*** (**A**) *CheWnt3*
926 relative gene expression using total mRNA samples of 1-day planula after
927 electroporation. *CheEF1a* was used as an internal control. Bar heights represent the
928 mean value of at least three independent experiments. Error bars indicate standard
929 deviation. siNC, siRNA universal negative control. (**B**) Percentage of "normal
930 phenotype" of 1-day planula after *CheWnt3* knockdown. Number of examined planula:
931 shRNA 400 ng/μl, n=288; siNC 400 ng/μl, n=45. Data are the average of three
932 biologically different experiments. Note that the same dataset for 0 and 400 ng/μl from
933 Fig. 4K and 4L were shown for comparison.
934
935
936 **Supplementary Figure 5. Phylogenetic analysis of *Cladonema* Wnt proteins.** To
937 analyze orthology of *Cladonema* Wnt proteins, phylogenetic analysis was performed by
938 using amino acids sequences of Wnt proteins from *Cladonema*, *Clytia* and
939 *Nematostella*. Maximum likelihood (ML) tree calculation was inferred on ClustalW with
940 the PhyML bootstrap method. Branch supports were computed out of 100 bootstrapped
941 trees. Tree was visualized using MEGA-X software (Kumar S, Stecher G, Li M, Knyaz
942 C, and Tamura K (2018) *Molecular Biology and Evolution* 35:1547-1549). We performed
943 *Cladonema* Wnt ligand CDS annotation using *Clytia* CDS database (MARIMBA, Marine
944 models database: http://marimba.obs-vlfr.fr) and found eight contigs annotated with Wnt
945 ligands in *Cladonema*. Among the eight Wnt contigs, CpWntX4
946 (TRINITY_DN27620_c1_g1_i1.p1) is homologous to the *Clytia* Wnt ligand CDS,
947 CheWntX4 (TCONS_00027333-protein), which has never been registered in GenBank.
948 We used protein BLAST, but no other homologous cnidarian Wnt was found, so that we
949 provide the name CpWntX4 for convenience.
950 *Cp, Cladonema pacificum; Che, Clytia hemisphaerica; Nv, Nematostella vectensis.*
951 GenBank accession numbers, transcriptome name or RNAseq contig ID are follows;
952 CpWnt5a (TRINITY_DN3183_c0_g3_i1.p1), CpWntX1A

953 (TRINITY_DN4292_c0_g1_i3.p1), CpWnt2 (TRINITY_DN8519_c0_g1_i1.p1), CpWnt9
954 (TRINITY_DN3403_c0_g1_i3.p1), CpWntX4 (TRINITY_DN27620_c1_g1_i1.p1),
955 CpWntX2 (TRINITY_DN13473_c0_g1_i3.p1), CpWnt7b
956 (TRINITY_DN9745_c0_g1_i1.p1), CheWnt2 (TCONS_00012270), CheWntX1A
957 (ACB15464.1), CheWnt3 (ACB15465.1), CheWntX4 (TCONS_00027333-protein),
958 CheWntX1B (TCONS_00065525), Wnt5 (ACB15462.1), CheWnt5a
959 (TCONS_00047033), CheWntX3 (ACB28461.1), CheWntX2 (ACB15461.1), CheWnt7b
960 (TCONS_00073720), CheWnt9 (TCONS_00056741), NvWnt1 (AAT00640.1), NvWnt3
961 (ABF48092.1), NvWnt5 (AAW28133.1), NvWnt6 (AAW28134.1)
962
963
964 **Supplementary Table 1**. **Survival rate of *Cladonema* embryos after**
965 **electroporation.** The number of cleavage stage *Cladonema* embryos at 1 h post
966 fertilization (hpf) was considered embryo survival. Compared to fertilized eggs,
967 unfertilized eggs were much less tolerant of electroporation.
968
969
970 **Supplementary Table 2**. **Survival rate of *Nematostella* embryos after**
971 **electroporation.** The number of live *Nematostella* larvae was counted at 3 dpf (planula
972 stage). The survival rate remained around 20-40% regardless of the difference in siRNA
973 concentration and target.
974
975

Figure 1

Masuda-Ozawa et al.

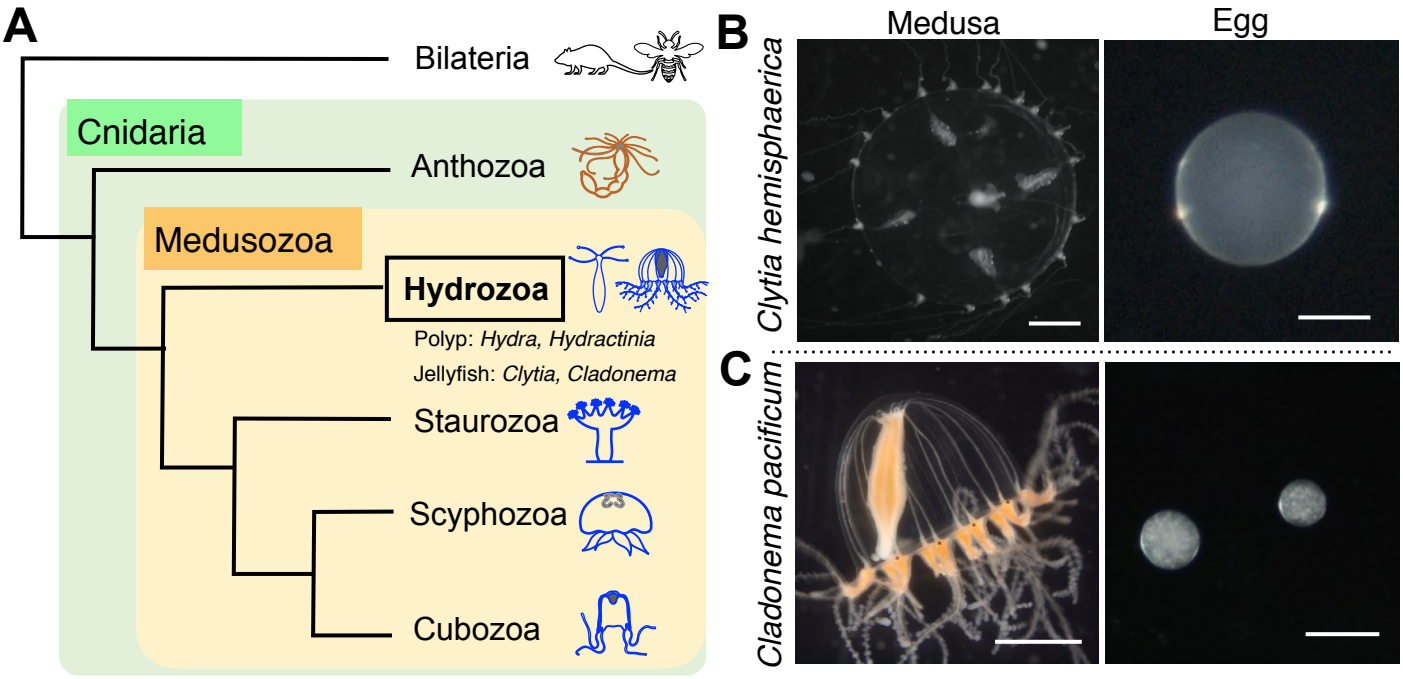

Figure 2

Masuda-Ozawa et al.

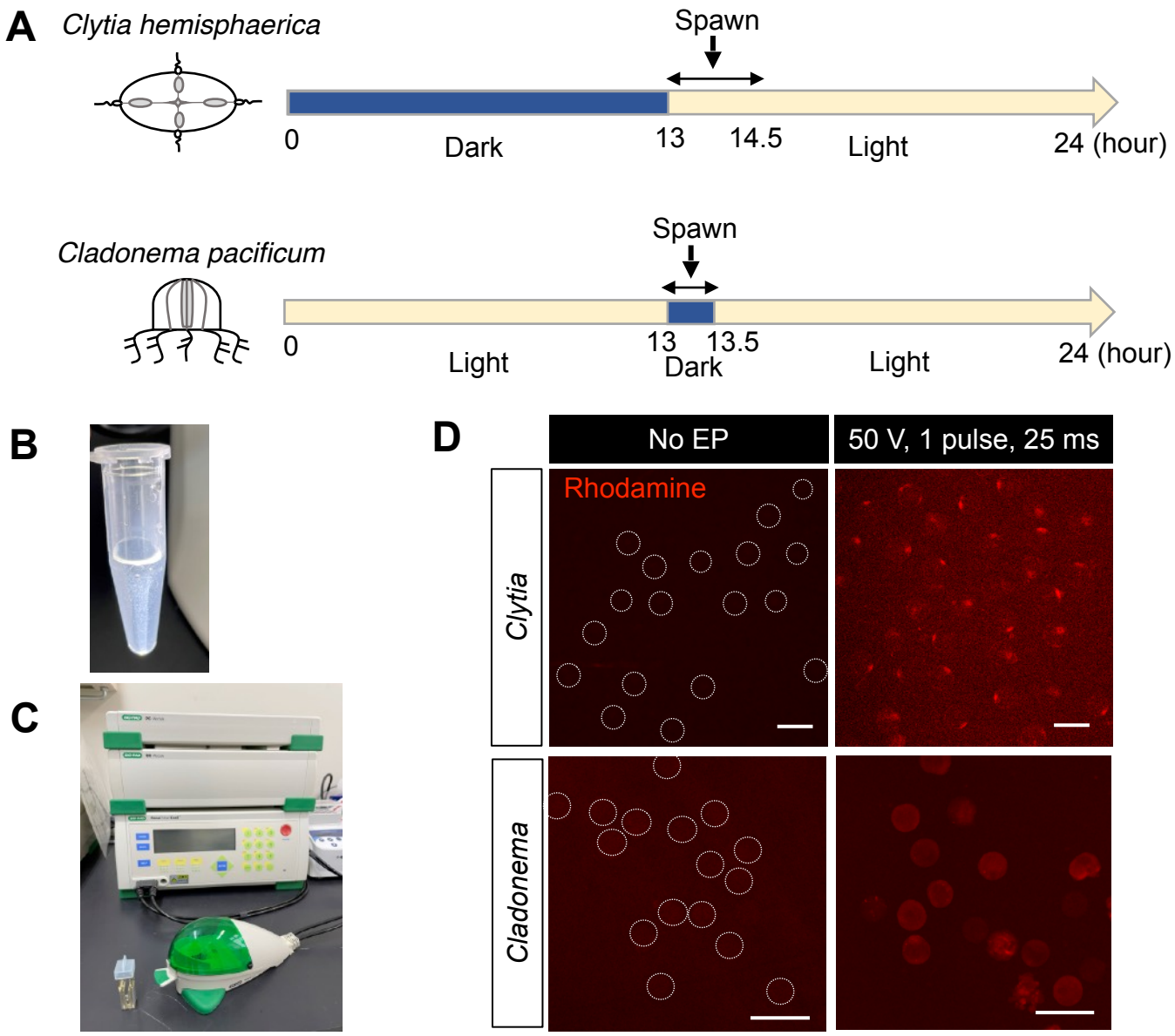

Figure 3

Masuda-Ozawa et al.

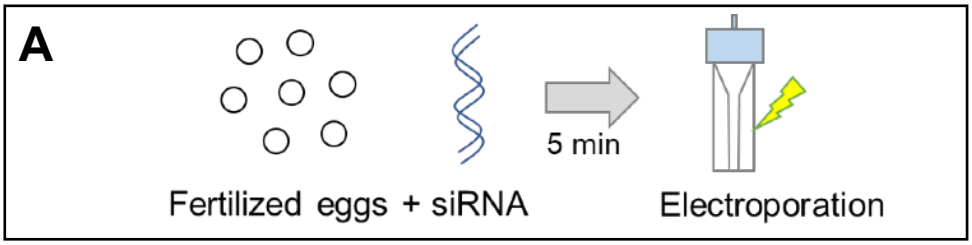

si*CheGFP1* electroporation
2 day planula

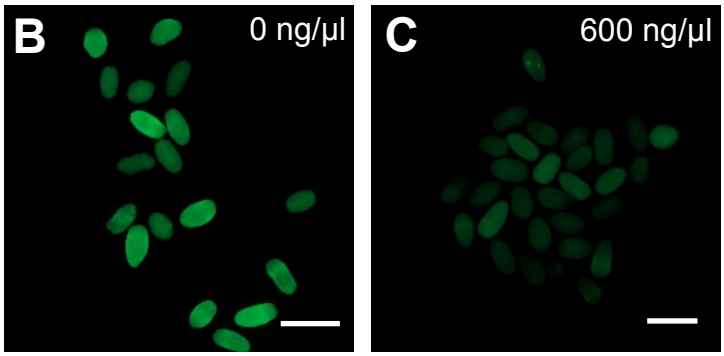

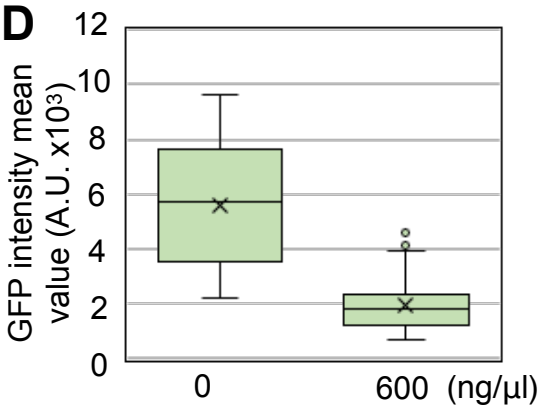

si*CheGFP1* electroporation/3 day planula

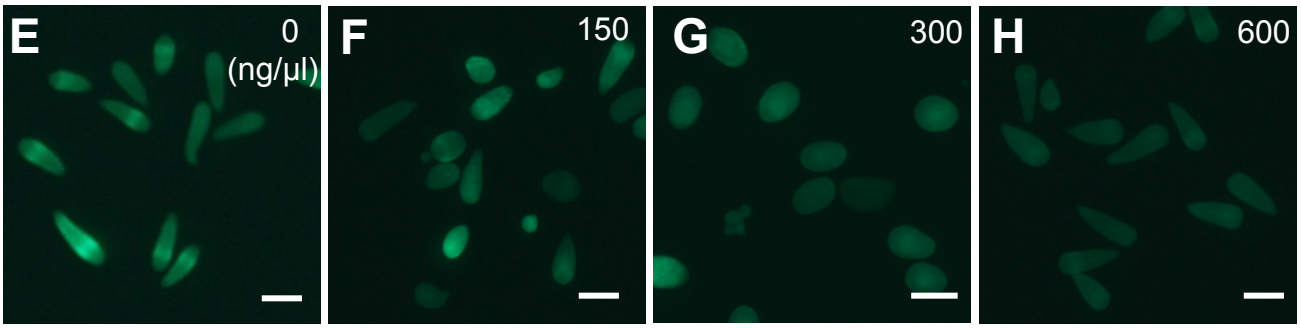

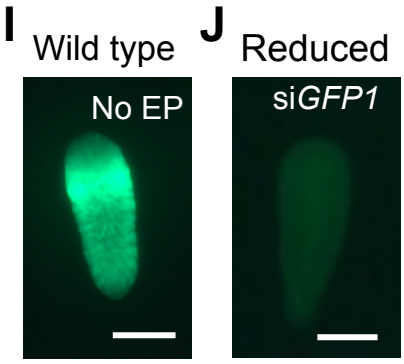

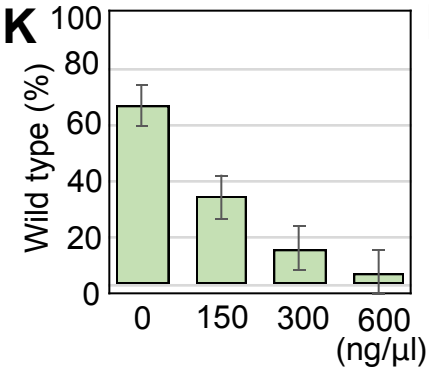

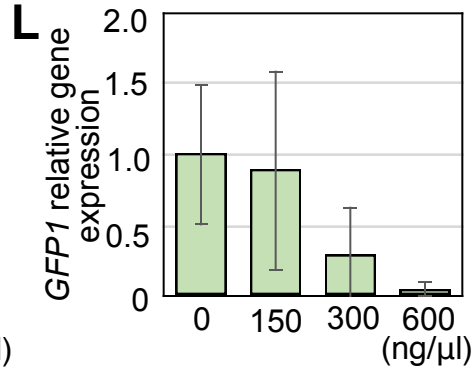

Figure 4

Masuda-Ozawa et al.

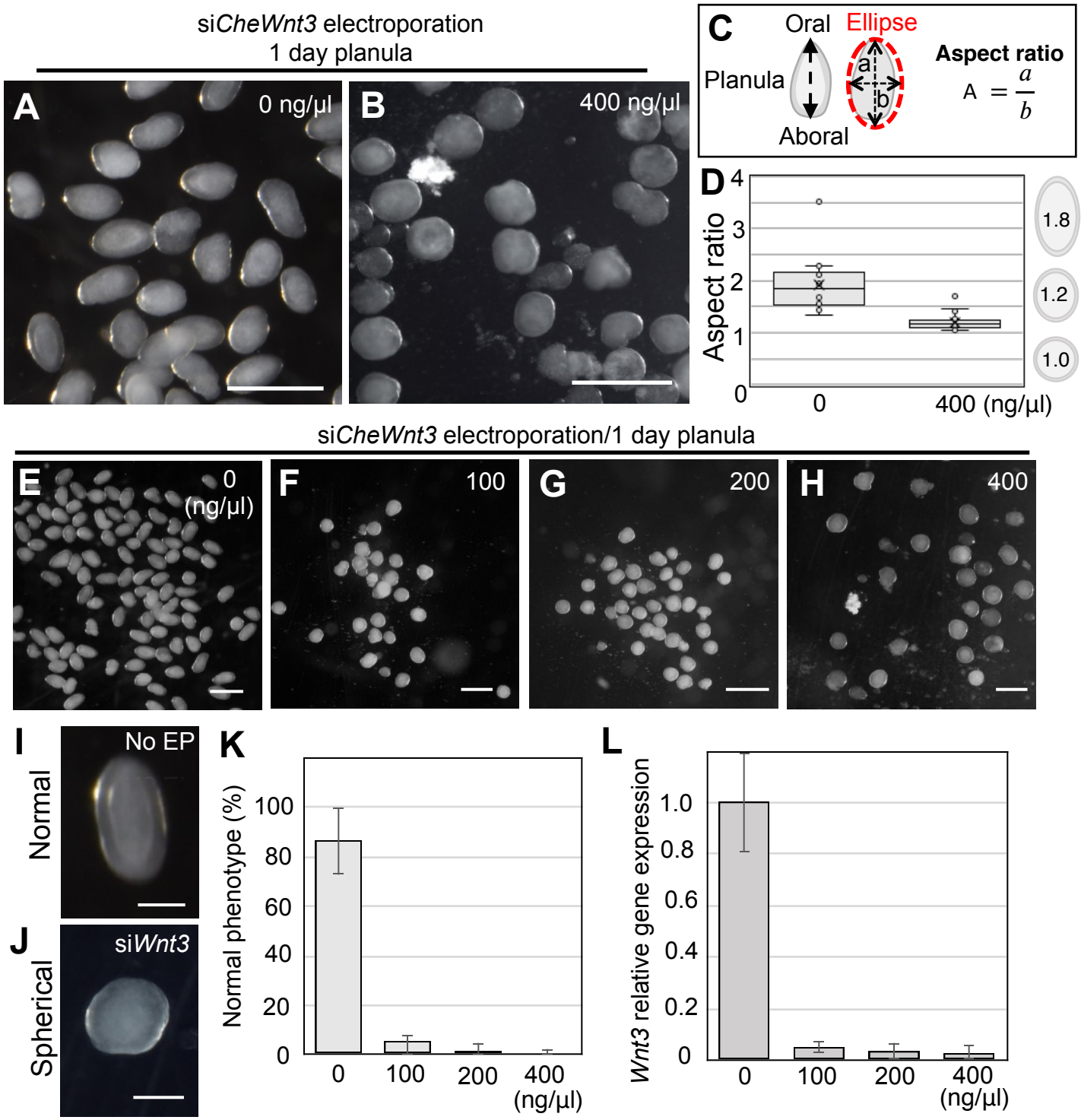

Figure 5

Masuda-Ozawa et al.

A

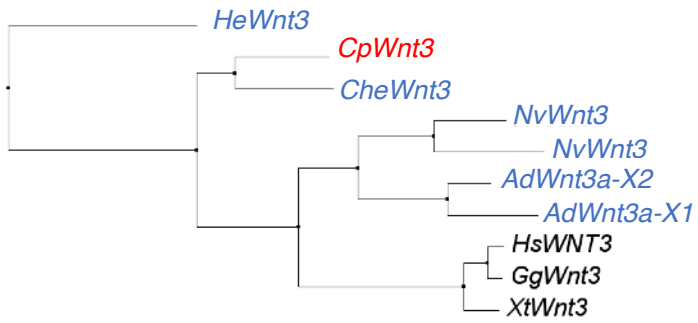

B

```
CpWnt3     61 CYNFTDLIPSVAEGVRLSIDECQEQFRNRKWNCSVSEEENSVFGPMISTASRESAFISGITSAGVAYAVTEACAEGKSVHCR 142
HeWnt3     60 CWNYTDLIRSVGEGVRLSIDECQEQFRYRKWNCSIGKK-GSVFGPMIRKASRESAFISGITSAGVAFAVTEACAEGRSMHCR 140
CheWnt3    56 CNNFTDLIPSVAEGIRLSIEECQEQFQTRKWNCSIMAGGNSIFGPMLQKASRESAFISGITAAGVAFSVTEACAEGRSLHCR 137
HsWNT3     59 CRNYIEIMPSVAEGVKLGIQECQHQFRGRRWNCTTIDDSLAIFGPVLDKATRESAFVHAIASAGVAFAVTRSCAEGTSTICG 140
GgWnt3     59 CRNYIEIMPSVAEGVKLGIQECQHQFRGRRWNCTTIDDSLAIFGPVLDKATRESAFVHAIASAGVAFAVTRSCAEGTSTICG 140
XtWnt3     58 CRNYIEIMPSVAEGIKLGIQECQHQFRGRRWNCTTIHDSLAIFGPVLDKATRESAFVHAIASAGVAFAVTRSCAEGSSTICG 139
NvWnt3     56 CRKNPDLMEHVAHGAKYGVHECRHQFRNRRWNCSTIRESGSLFESVLSKGCREAAFVHAVTAAGVAHSVTDACSKGRIESCD 137
NvWnt3a    17 CRKNPDLMEHVAHGAKYGVHECRHQFRNRRWNCSTIRESGSLFESVLSKGCREAAFVHAVTAAGVAHSVTDACSKGRIESCD  98
AdWnt3a-X2 56 CRKHPTLMTSVAKGVKDAVEECQIQFERRRWNCSAVPESGTLFDPILKRASREAAYLHAITAAGVSHAVTASCGEGNLQSCD 137
AdWnt3a-X1 83 CRKHPTLMTSVAKGVKDAVEECQIQFERRRWNCSAVPESGTLFDPILKRASREAAYLHAITAAGVSHAVTASCGEGNLQSCD 164

CpWnt3    143 CDNSIRGQT-DEGWRWGGCNRPISYGIWFSQLFIDQVEHLMKKRRHPRKFMNLHNNRAGREIIRHNLATKCKCHGMSGNCNL 223
HeWnt3    141 CDNSIRGKT-EAGWQWGGCNRPISYGIWFSKLFIDQVEVLTRKKRHPRKQMNLHNNQAGREIIRNNLATRCKCHGMSGNCNV 221
CheWnt3   138 CDNSIRGQT-EEGWKWGGCNRPISYGIWFSQLFIDMVEIKVKKRRDPRRAMNLHNNRAGREIIRHNLATKCKCHGMSGNCNL 218
HsWNT3    141 CDSHHKGPP-GEGWKWGGCSEDADFGVLVSREFADARENRP----DARSAMNKHNNEAGRTTILDHMHLKCKCHGLSGSCEV 217
GgWnt3    141 CDSHHKGPP-GEGWKWGGCSEDADFGVLVSREFADARENRP----DARSAMNRHNNEAGRTTILDHMHLKCKCHGLSGSCEV 217
XtWnt3    140 CDSHHKGSP-GDGWKWGGCSEDADFGVLVSREFADARENRP----DARSAMNRHNNEAGRATILDHMHLRCKCHGLSGSCEV 216
NvWnt3    138 CDRNLSGRS-SKGWTWSGCNSNIKFGVWFSKQFTEARERGD----DLRQIMNRHNSRAGRKALEELVARKYKCHGLSGSCSM 214
NvWnt3a    99 CDRNLSGRS-SKGWTWSGCNSNIKFGVWFSKQFTEARERGG----DLRQIMNRHNSRAGRKALEELVARKCKCHGLSGSCSM 175
AdWnt3a-X2 138 CDRSLSGTATQKGWTWSGCSSNVKFGTWFSEQFTDASTKGN----SPRAVMNRHNSRAGRKALSRLLARKCKCHGLSGSCTM 215
AdWnt3a-X1 165 CDRSLSGTATQKGWTWSGCSSNVKFGTWFSEQFTDASTKGN----SPRAVMNRHNSRAGRKALSRLLARKCKCHGLSGSCTM 242

CpWnt3    224 KTCWLAQPKFSEIGRLLKDRYDSAHEMMHEFKVKKNKKKKFKRLVPKYKEYLPPSTLDFIYYEESPDYCVDNKMLGLSGTKG 305
HeWnt3    222 KTCWLAQPKFPEIGKKLKDRYDSAHEMEFEY-------------------------------------------------- 252
CheWnt3   219 KTCWLAQPGFQQLGKMLKDRYDSAHEMDFEFKIKKNGKKRFKKLIPRYKEYLPPSTLDFVYYEESPNYCENNNSLGIIGTRG 300
HsWNT3    218 KTCWWAQPDFRAIGDFLKDKYDSASEMVVEKHR--ESRGWVETLRAKYSLFKPPTERDLVYYENSPNFCEPNPETGSFGTRD 297
GgWnt3    218 KTCWWAQPDFRAIGDYLKDKYDSASEMVVEKHR--ESRGWVETLRAKYALFKPPTERDLVYYENSPNFCEPNPETGSFGTRD 297
XtWnt3    217 KTCWWSQPDFRAIGDHLKDKYDSASEMSVEKHR--ESRGWVETLRAKYSLFKPPTERDLVYYETSPNFCEPNPETGSFGTQG 296
NvWnt3    215 KTCWMQQANFRQIGDHLKVKYDSAVEMTTKVNR--RGK---KRLKPKYSHFKKPSDKDLIYFETSPNYCDKNVTVGSLGTSG 291
NvWnt3a   176 KTCWMQQANFRQIGDHLKVKYDSAVEMTTKVNR--RGK---KRLKPKYSHFKKPSDKDLIYFETSPNYCDKNVTVGSLGTSG 252
AdWnt3a-X2 216 KTCWMQQPTFHQVGDHLKKKYESASEMVVKLNR--RGK---ERLRLRHNHLKRPSESDLMYYEPSPNYCDRDPSEGSLGTSG 292
AdWnt3a-X1 243 KTCWMQQPTFHQVGDHLKKKYESASEMVVKLNR--RGK---ERLRLRHNHLKRPSESDLMYYEPSPNYCDRDPSEGSLGTSG 319

CpWnt3    306 RECNITSSSVDGCELMCCNRGYNVDIVQETKSGKGKFIWCCQVQCQKCTQAVAKYTCK                         363
HeWnt3      ------------------------------------------------------------
CheWnt3   301 RECNITSAGVDGCDQMCCRRGFNVKIVQETKAGDGKFIWCCHVKCKKCTEAVPRYTCK                         358
HsWNT3    298 RTCNVTSHGIDGCDLLCCGRGHNTRTEKRKEKCHCIFHWCCYVSCQECIRIYDVHTCK                         355
GgWnt3    298 RTCNVTSHGIDGCDLLCCGRGHNTRTEKRKEKCHCIFHWCCYVSCQECIRVYDVHTCK                         355
XtWnt3    297 RSCNVTSHGIDGCDLLCCGRGHNTRTEKRKEKCHCIFHWCCYVSCQECVRIYDVHTCK                         354
NvWnt3    292 RQCNYTSNGIDGCELLCCGRGHNIQQAKITRNCNCVFKWCCEVKCERCKEV-------                         342
NvWnt3a   253 RQCNYTSNGIDGCELLCCGRGHNIQQAKITRNCNCVFKWCCEVKCERCKEVVNIYTCK                         310
AdWnt3a-X2 293 RECNISSSGIDGCELLCCGRGHNIQQVKVTRNCNCIFIWCCHVKCQKCKEIVNKYTCK                         350
AdWnt3a-X1 320 RECNISSSGIDGCELLCCGRGHNIQQVKVTRNCNCIFIWCCHVKCQKCKEIVNKYTCK                         377
```

Figure 6
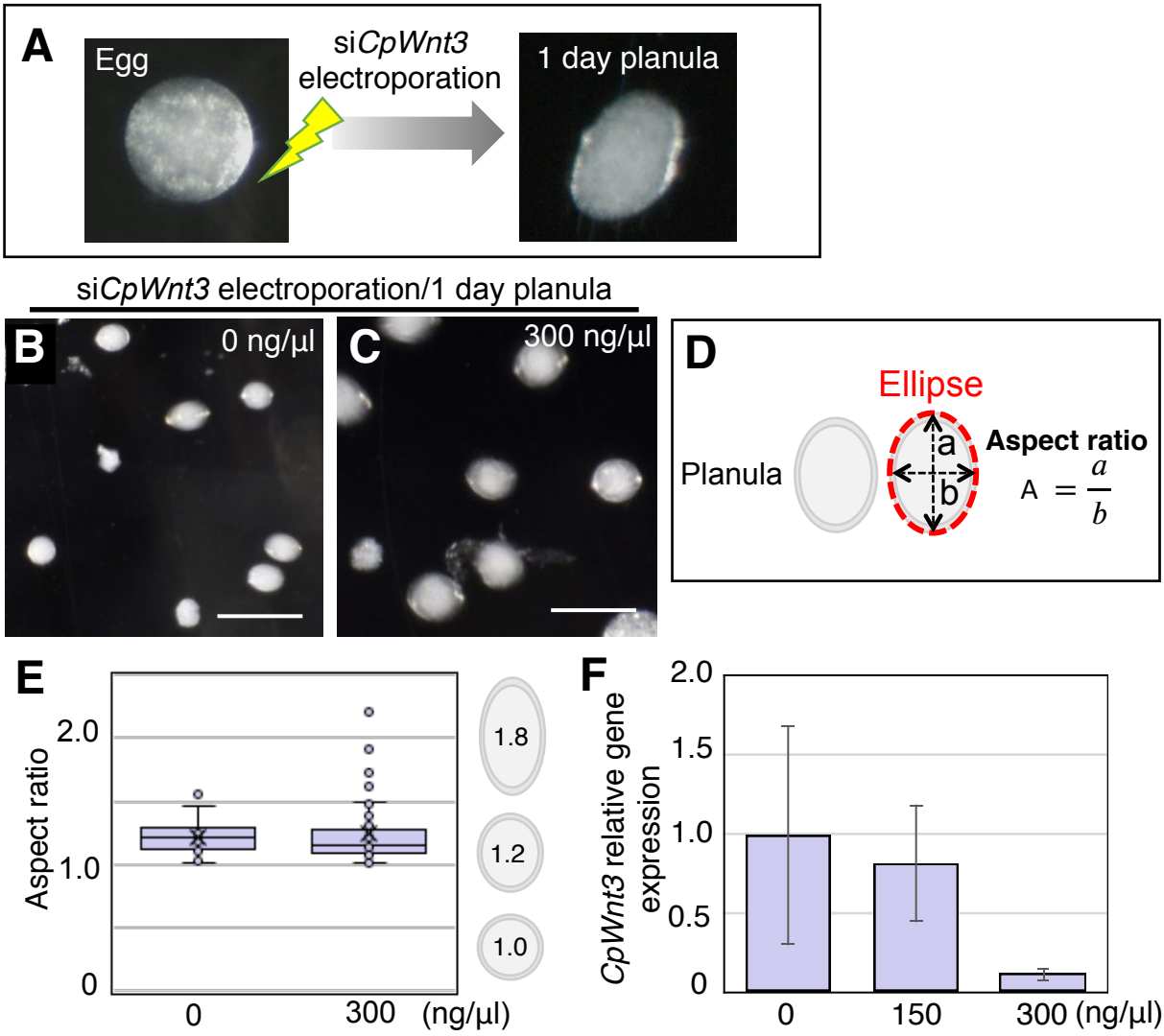
Masuda-Ozawa et al.